

# A STREAMLINE UPWIND PETROV-GALERKIN REDUCED ORDER METHOD FOR ADVECTION-DOMINATED PARTIAL DIFFERENTIAL EQUATIONS UNDER OPTIMAL CONTROL

FABIO ZOCCOLAN<sup>1</sup>, MARIA STRAZZULLO<sup>2</sup>, AND GIANLUIGI ROZZA<sup>3</sup>

**ABSTRACT.** In this paper we will consider distributed Linear-Quadratic Optimal Control Problems dealing with Advection-Diffusion PDEs for high values of the Péclet number. In this situation, computational instabilities occur, both for steady and unsteady cases. A Streamline Upwind Petrov-Galerkin technique is used in the optimality system to overcome these unpleasant effects. We will apply a finite element method discretization in a *optimize-then-discretize* approach. For the parabolic case, a space-time framework will be considered and stabilization will also occur in the bilinear forms involving time derivatives. Then we will build Reduced Order Models on this discretization procedure and two possible settings can be analyzed: whether or not stabilization is needed in the online phase, too. In order to build the reduced bases for state, control, and adjoint variables we will consider a Proper Orthogonal Decomposition algorithm in a partitioned approach. The discussion is supported by computational experiments, where relative errors between the FEM and ROM solutions are studied together with the respective computational times.

## 1. INTRODUCTION

The main goal of *Optimal Control* theory is to modify a physical or engineering system through an input, called *control*, to obtain a desired *output*. From a theoretical point of view, one can describe the state problem through partial differential equations (PDEs), following the approach of J.L. Lions [30, 31]. Applying an optimal control means to solve a constrained optimization problem, where a cost functional has to be minimized. This process translates into an optimality system, which will be discretized for numerical simulations, that, in this framework, are more and more needed. Thus, effective and fast numerical techniques are required to exploit optimal control in scientific and industrial applications.

In this work, we will consider Advection-Diffusion equations [42] for large Péclet numbers. These equations are widespread in many engineering contexts since they can model transfer of particles, of energy, of heat and so on. In the case of high values of the Péclet number, numerical instabilities occur during discretization: this can happen for related optimal control problems, too. Thus, it becomes necessary to introduce some stabilization techniques to overcome this undesired behaviour. We exploit a Streamline Upwind Petrov-Galerkin (SUPG) technique over a finite element method (FEM) [11, 26, 38] in a *optimize-then-discretize* approach, as done in [14], to provide strongly-consistency to the discretization. When we deal with unsteady problems, a space-time discretization [21, 46, 50, 51, 52, 57] will be used together with the SUPG stabilization for bilinear forms related to the derivative over time. The discretization procedure can easily request a huge amount of computational resources, especially for parametric time-dependent problems. The parameters can represent physical or geometrical features of the system at hand. In this scenario, we decide to exploit the parameter dependence of the equations to build Reduced Order Models (ROMs) [22, 40, 39, 43] by means of Proper Orthogonal Decomposition (POD) algorithm in a partitioned approach. Namely,

<sup>1</sup> SECTION DE MATHÉMATIQUES, ÉCOLE POLYTECHNIQUE FÉDÉRALE DE LAUSANNE, 1015 LAUSANNE, SWITZERLAND, EMAIL: FABIO.ZOCCOLAN@EPFL.CH

<sup>2</sup> DISMA, POLITECNICO DI TORINO, CORSO DUCA DEGLI ABRUZZI 24, TURIN, ITALY. EMAIL: MARIA.STRAZZULLO@POLITO.IT

<sup>3</sup> MATHLAB, MATHEMATICS AREA, SISSA, VIA BONOMEA 265, I-34136 TRIESTE, ITALY. EMAIL: GIANLUIGI.ROZZA@SISSA.IT

the discretization process is divided in two phases: an *offline* stage where a low-dimensional space is built through FEM solutions computed in properly chosen parameters, and an *online* stage, where the system is solved for a new parametric instance in the new low-dimensional framework. Thus, we consider two possible strategies: the former is to stabilize the system only in the offline phase; the latter uses SUPG in the online one, too. This setting was considered for problems without optimal control in [37, 55]. To the best of our knowledge, it is the first time that SUPG stabilization for time-dependent Advection-Dominated problems under distributed control is analyzed in a ROM setting.

This work is organized as follows. The first section will illustrate some theoretical aspects about Optimal Control Theory for PDEs. Section 3 shows the FEM discretization that will be used for numerical experiments, an introduction to Advection-Dominated problems, and SUPG technique in an *optimize-then-discretize* approach. Instead, in Section 4, we will focus on the ROM setting and Section 5 refers to the related numerical simulations. Firstly, we will introduce two specific examples of Advection-Diffusion problems: the Graetz-Poiseuille and the Propagating Front in a Square Problems. The former was studied in various forms without optimal control in [18, 37, 44, 55] and with optimal control but without stabilization in [34, 50]. The latter is studied without optimal control in a similar version in [37, 55]. Here, both the problems will be analyzed under a distributed optimal control for high values of the Péclet number, both in the steady and unsteady cases. Relative errors between FEM and ROM solutions will be shown, as well as an analysis on the computational times.

## 2. PROBLEM FORMULATION

In this Section we will illustrate the fundamentals of Linear-Quadratic Optimal Control Problem (OCP) for steady and unsteady PDEs. The aim of Optimal Control is to achieve a prescribed optimality condition by minimizing a suitable cost functional under the constraint of satisfying the PDE Problem. The proposed framework follows the J.L. Lions theory [30, 31].

**2.1. Parametric Optimal Control Problems governed by PDEs.** The main features of an OCP are:

- (1) a controlled system, i.e. an input-output process given by a system of PDEs;
- (2) the output of the system, or an observation of it, when the output cannot be measured directly. In our case, we will consider the solution of the system as the output;
- (3) a control, which constitutes the input of the system. It influences the output which can be expressed as a function of it. In this work we will only consider distributed control;
- (4) an objective condition to be fulfilled, which can be represented by a real functional.

Therefore, from a mathematical perspective, we can state that an OCP is characterized by:

- $e$ , the *state equation function*, which expresses the relationship between the output and the control within the system in terms of a PDE problem or PDEs in a weak formulation. A pair  $(y, u) \in X := Y \times U$  is said to be *physical* or *feasible* if it is a solution of the state equation  $e$ ;  $y$  is called the *state variable*, *the output*, and  $u$  is the control variable, *the input*.  $X_{ad}$  is the set of all the feasible pairs  $(y, u)$ ;
- $z(y) = Oy$ , a direct *observation* of the output. Here, a linear operator  $O$  is applied to the state to describe the observation: we will denote the space of observation as  $Z$ . We will only deal with state variables that can be measured on a portion of the domain;
- $J$ , the *objective functional*, which describes the objective to achieve.
- suitable spaces  $Y$  and  $U$ , as the *state space* and *control space* respectively. Domains of definition for control and/or state can be taken smaller due to possible restrictions; hence we have to introduce  $Y_{ad} \subseteq Y$  and  $U_{ad} \subseteq U$  as the *admissible state space* and *admissible control space* respectively. However, we will always consider *unconstrained problems*, i.e.  $X_{ad} = X$ . The theory of well-posedness can make use of the Lagrangian approach as in [12, 34] or it can be consider as a particular case of the general Adjoint approach when we can deal with  $X_{ad} \subset Y_{ad} \times U_{ad}$  [24, 30, 38].

Let us consider  $\Omega \subset \mathbb{R}^n$ , an open and bounded regular domain, and the time interval  $(0, T) \subset \mathbb{R}^+$ : for us it will always be the case of  $n = 2$ . Let us denote with  $\Gamma_D$  and  $\Gamma_N$  the portions of the boundary of  $\partial\Omega$  where Dirichlet and Neumann boundary conditions are specified, respectively. We define the *observation domain*  $\Omega_{obs} \subseteq \Omega$  as the portion of the domain where we want that the state variable assumes a desired value.  $\mathcal{P} \subseteq \mathbb{R}^p$ , for natural number  $p$ , is the parameter space and  $\boldsymbol{\mu} \in \mathcal{P}$  is a  $p$ -vector which can represent physical or geometrical parameter of interest. In this work we deal with *Parametric Optimal Control Problems* (OCP( $\boldsymbol{\mu}$ )s), i.e. systems where there is a dependency on the parameter  $\boldsymbol{\mu}$ .

**Problem 2.1.1** (Parametric Optimal Control Problem). *Given  $Y, U$  real Banach spaces, consider the state equation  $e : Y \times U \rightarrow Q$ , with  $Q$  a Banach space, which fulfills a set of boundary and/or initial conditions, and the objective functional  $J : Y \times U \rightarrow \mathbb{R}$ . Given  $\boldsymbol{\mu} \in \mathcal{P}$ , then find  $(y(\boldsymbol{\mu}), u(\boldsymbol{\mu})) \in X$  such that the cost functional  $J(y(\boldsymbol{\mu}), u(\boldsymbol{\mu}); \boldsymbol{\mu})$  is minimized subject to  $e(y(\boldsymbol{\mu}), u(\boldsymbol{\mu}); \boldsymbol{\mu}) = 0$ .*

**2.2. Lagrangian Approach.** We refer to the Lagrangian approach to state the well-posedness of OCP( $\boldsymbol{\mu}$ )s in *full admissibility* setting, i.e. when  $X_{ad} = Y \times U$ . We want to solve:

$$\min_{(y(\boldsymbol{\mu}), u(\boldsymbol{\mu})) \in Y \times U} J(y(\boldsymbol{\mu}), u(\boldsymbol{\mu}); \boldsymbol{\mu}) \text{ s.t. } e(y(\boldsymbol{\mu}), u(\boldsymbol{\mu}); \boldsymbol{\mu}) = 0,$$

thus we define the Lagrangian operator  $\mathcal{L} : Y \times U \times Q^* \rightarrow \mathbb{R}$  as:

$$(1) \quad \mathcal{L}(y(\boldsymbol{\mu}), u(\boldsymbol{\mu}), p(\boldsymbol{\mu}); \boldsymbol{\mu}) = J(y(\boldsymbol{\mu}), u(\boldsymbol{\mu}); \boldsymbol{\mu}) + \langle p(\boldsymbol{\mu}), e(y(\boldsymbol{\mu}), u(\boldsymbol{\mu}); \boldsymbol{\mu}) \rangle_{Q^*Q},$$

where  $p(\boldsymbol{\mu})$  is a Lagrange multiplier belonging to  $Q^*$ , the dual space of  $Q$ . For the sake of notation, we write  $y := y(\boldsymbol{\mu})$ ,  $u := u(\boldsymbol{\mu})$  and  $p := p(\boldsymbol{\mu})$ : we will explicit the parameter dependence only when necessary. The discussion inherent to the Lagrangian approach is based on [12], the same reference presents a comparison between this approach and the adjoint one. For the sake of simplicity, we make some regularity assumptions [12]:

**Assumption 2.2.1.** *The objective functional  $J$  and the state equation  $e$  are Fréchet differentiable, more precisely the differential operator related to  $J$  is continuous, i.e.  $J'(\boldsymbol{\mu}) \in C(Y \times U, \mathcal{B}(Y \times U, \mathbb{R}))$ , where  $\mathcal{B}(\bar{V}, \hat{V})$  is the space of linear bounded operators between Banach spaces  $\bar{V}$  and  $\hat{V}$ .*

The following theorem and proposition claim that under Assumption 2.2.1 minimizers of the function  $J$ , subject to equality constraints  $e$ , can be critical points of (1) [53].

**Theorem 2.2.2** (Lagrange Multipliers). *Let  $X := Y \times U$  and  $V \subseteq X$  be an open subset such that  $J$  and  $e$  are Fréchet differentiable on  $V$ . Assume  $x = (y, u) \in V$  to be a minimizer of  $J$  subject to the constraint  $e(x; \boldsymbol{\mu}) = 0$ , and  $e'(x; \boldsymbol{\mu}) \in \mathcal{B}(X, Q)$  to be surjective. Then, there exists a Lagrange multiplier  $p \in Q^*$  such that  $(x, p)$  is an unconstrained stationary point of the Lagrangian  $\mathcal{L}$  in (1).*

Therefore, in order to find a stationary point  $(y, u, p)$  of  $\mathcal{L}$ , one has to solve the following optimality system [12]:

$$(2) \quad \begin{cases} \mathcal{L}_y(y, u, p; \boldsymbol{\mu})(\bar{y}) = J_y(y, u; \boldsymbol{\mu})(\bar{y}) + \langle p, e_y(y, u; \boldsymbol{\mu})(\bar{y}) \rangle_{Q^*Q} = 0, & \forall \bar{y} \in Y, \\ \mathcal{L}_u(y, u, p; \boldsymbol{\mu})(\bar{u}) = J_u(y, u; \boldsymbol{\mu})(\bar{u}) + \langle p, e_u(y, u; \boldsymbol{\mu})(\bar{u}) \rangle_{Q^*Q} = 0, & \forall \bar{u} \in U, \\ \mathcal{L}_p(y, u, p; \boldsymbol{\mu})(\bar{p}) = \langle \bar{p}, e(y, u; \boldsymbol{\mu}) \rangle_{Q^*Q} = 0, & \forall \bar{p} \in Q^*. \end{cases}$$

In the Lagrangian formulation  $Q^*$  is said the *adjoint space*. The above result easily implies the following useful proposition [38], where we derive another system of three equations that we will use in the numerical simulations.

**Proposition 2.2.3** (Optimality System). *Suppose  $X_{ad} = Y \times U$  and Assumption 2.2.1 holds, then for some  $p \in Q^*$  a minimizer  $x = (y, u)$  of 2.1.1 where  $e'(y, u; \boldsymbol{\mu})$  is surjective must satisfy*

$$(3) \quad \begin{cases} \mathcal{L}_y(y, u, p; \boldsymbol{\mu}) = J_y(y, u; \boldsymbol{\mu}) + e_y(y, u; \boldsymbol{\mu})^* p = 0, & \text{in } Y^*, \\ \mathcal{L}_u(y, u, p; \boldsymbol{\mu}) = J_u(y, u; \boldsymbol{\mu}) + e_u(y, u; \boldsymbol{\mu})^* p = 0, & \text{in } U^*, \\ \mathcal{L}_p(y, u, p; \boldsymbol{\mu}) = e(y, u; \boldsymbol{\mu}) = 0, & \text{in } Q. \end{cases}$$

In (3), the first equation is called the *adjoint equation*, the second one is the *gradient equation* and, as we have already seen, the *state equation* is the third one. We remark that we will always consider Linear-Quadratic problems.

**Definition 2.2.4** (Linear-Quadratic Problem). *Consider a Banach space  $Z$  and  $\alpha > 0$ . Let the Observation map  $O : Y \rightarrow Z$  be a linear and bounded operator. Consider an element  $z_d(\boldsymbol{\mu}) \in Z$ , which is the so-called desired solution profile (the desired observed output). Let  $J$  be a quadratic objective functional of the form*

$$(4) \quad J(y, u; \boldsymbol{\mu}) = \frac{1}{2}m(Oy(\boldsymbol{\mu}) - z_d(\boldsymbol{\mu}), Oy(\boldsymbol{\mu}) - z_d(\boldsymbol{\mu})) + \frac{\alpha}{2}n(u(\boldsymbol{\mu}), u(\boldsymbol{\mu})),$$

where  $m : Z \times Z \rightarrow \mathbb{R}$  and  $n : U \times U \rightarrow \mathbb{R}$  are symmetric and continuous bilinear forms. Let  $e$  be affine, i.e. there exist  $A(\boldsymbol{\mu}) \in \mathcal{B}(Y, Q)$ ,  $B(\boldsymbol{\mu}) \in \mathcal{B}(U, Q)$  and  $f(\boldsymbol{\mu}) \in Q$  such that

$$(5) \quad e(y, u; \boldsymbol{\mu}) = A(\boldsymbol{\mu})y + B(\boldsymbol{\mu})u - f(\boldsymbol{\mu}), \quad \forall (y(\boldsymbol{\mu}), u(\boldsymbol{\mu})) \in Y \times U.$$

Then an OCP( $\boldsymbol{\mu}$ )s with the above properties is said a Linear-Quadratic Optimal Control Problem.

For Linear-Quadratic OCP( $\boldsymbol{\mu}$ )s Proposition 2.2.3 implies that a solution  $(y, u)$  to Problem 2.1.1 must satisfy, for some  $p \in Q^*$  [12],

$$(6) \quad \begin{cases} m(Oy, O\bar{y}; \boldsymbol{\mu}) + \langle A^*(\boldsymbol{\mu})p, \bar{y} \rangle_{Y^*Y} = m(O\bar{y}, z_d; \boldsymbol{\mu}), & \forall \bar{y} \in Y, \\ \alpha n(u, \bar{u}; \boldsymbol{\mu}) + \langle B^*(\boldsymbol{\mu})p, \bar{u} \rangle_{U^*U} = 0, & \forall \bar{u} \in U, \\ \langle \bar{p}, A(\boldsymbol{\mu})y + B(\boldsymbol{\mu})u \rangle_{Q^*Q} = \langle \bar{p}, f(\boldsymbol{\mu}) \rangle_{Q^*Q}, & \forall \bar{p} \in Q^*. \end{cases}$$

In this context, if  $(y, u, p)$  is a saddle point of  $\mathcal{L}$  [56], then  $(y, u)$  minimizes  $J$  over all zeroes of  $e$  [12]. Moreover, under some precise hypotheses existence and uniqueness of a saddle point can be provided using Brezzi Theorem [9, 10, 12]. Therefore, a possible strategy to prove well-posedness of an Linear-Quadratic OCP( $\boldsymbol{\mu}$ )s can be to demonstrate that a stationary point of (6) is a saddle point. At this purpose, System (6) can also be recast in a saddle-point structure [7, 12, 36]. In order to derive this structure, assume  $x \in X := Y \times U$ . We define  $M(\boldsymbol{\mu}) \in \mathcal{B}(Z, Z^*)$ ,  $N(\boldsymbol{\mu}) \in \mathcal{B}(U, U^*)$  as the unique operators that satisfy the following relations:

$$\langle M(\boldsymbol{\mu})z, \bar{z} \rangle_{Z^*Z} = m(z, \bar{z}; \boldsymbol{\mu}), \quad \langle N(\boldsymbol{\mu})u, \bar{u} \rangle_{U^*U} = n(u, \bar{u}; \boldsymbol{\mu}), \quad \forall z, \bar{z} \in Z, \forall u, \bar{u} \in U.$$

This directly implies that  $m(Oy, O\bar{y}; \boldsymbol{\mu}) = \langle O^*M(\boldsymbol{\mu})Oy, \bar{y} \rangle_{Y^*Y}$ . Using Proposition (2.2.3) and a matrix notation as follows [12]:

$$(7) \quad E(\boldsymbol{\mu}) = \begin{pmatrix} A(\boldsymbol{\mu}) & B(\boldsymbol{\mu}) \end{pmatrix}, \quad D(\boldsymbol{\mu}) = \begin{pmatrix} O^*M(\boldsymbol{\mu})O & 0 \\ 0 & \alpha N(\boldsymbol{\mu}) \end{pmatrix}, \quad E^*(\boldsymbol{\mu}) = \begin{pmatrix} A^*(\boldsymbol{\mu}) \\ B^*(\boldsymbol{\mu}) \end{pmatrix},$$

defining also  $\bar{g}(\boldsymbol{\mu}) = O^*M(\boldsymbol{\mu})z_d$ , the optimality system (6) for Linear-Quadratic OCP( $\boldsymbol{\mu}$ )s can be written in a more compact form as

$$(8) \quad \begin{pmatrix} D(\boldsymbol{\mu}) & E^*(\boldsymbol{\mu}) \\ E(\boldsymbol{\mu}) & 0 \end{pmatrix} \begin{pmatrix} x \\ p \end{pmatrix} = \begin{pmatrix} \bar{g}(\boldsymbol{\mu}) \\ f(\boldsymbol{\mu}) \end{pmatrix} \quad \begin{array}{l} \text{in } X^*, \\ \text{in } Q. \end{array}$$

For Linear-Quadratic Problems, a saddle point of  $\mathcal{L}$  is a stationary point [56], so it satisfies (6). For Linear-Quadratic problems the solution to system (8), and hence to (6), is a saddle point of  $\mathcal{L}$  when  $D(\boldsymbol{\mu})$  is self-adjoint [12]. In this case Brezzi Theorem gives us well-posedness [9, 10, 12].

**Lemma 2.2.5.** [12] *If  $Y$  is reflexive so that  $D(\boldsymbol{\mu}) = D^*(\boldsymbol{\mu})$ , then  $(x, p) = (y, u, p)$  is a saddle point of  $\mathcal{L}$  if and only if it solves the system (8).*

**Assumption 2.2.6.** *We assume that  $Y, U$  are reflexive,  $A(\boldsymbol{\mu})$  is weakly coercive, the operator  $B(\boldsymbol{\mu})$  is not null,  $\alpha N(\boldsymbol{\mu})$  is coercive with constant  $\alpha > 0$  and  $m(z, z; \boldsymbol{\mu}) \geq 0$ ,  $\forall z \in Z$ .*

Considering Linear-Quadratic OCP( $\boldsymbol{\mu}$ )s and Assumption 2.2.6, it follows that  $E(\boldsymbol{\mu})$  is inf-sup stable and  $D(\boldsymbol{\mu})$  is coercive over the kernel of  $E(\boldsymbol{\mu})$ . Consequently, the well-posedness of the system (8) is assured by Theorem 2.2.7.

**Theorem 2.2.7** (Brezzi). [9, 10, 12] *Let  $X$  be a reflexive Banach space. Then the equivalence of the following statements holds:*

- (1)  $D(\boldsymbol{\mu}) \in \mathcal{B}(X, X^*)$ ,  $E(\boldsymbol{\mu}) \in \mathcal{B}(X, Q)$  with the following properties:
  - $D(\boldsymbol{\mu})$  is weakly coercive over the kernel of  $E(\boldsymbol{\mu})$ ,
  - $E(\boldsymbol{\mu})$  is inf-sup stable.
- (2) The system (8) has a unique solution  $(x, p) \in X \times Q^*$  for all  $\bar{g}(\boldsymbol{\mu}) \in X^*$ ,  $f(\boldsymbol{\mu}) \in Q$ , which satisfies for some constant  $C > 0$   $\|x\|_X + \|p\|_{Q^*} \leq C(\|\bar{g}(\boldsymbol{\mu})\|_{X^*} + \|f(\boldsymbol{\mu})\|_Q)$ .
- (3) The operator  $\mathcal{S}(\boldsymbol{\mu}) := \begin{pmatrix} D(\boldsymbol{\mu}) & E^*(\boldsymbol{\mu}) \\ E(\boldsymbol{\mu}) & 0 \end{pmatrix}$  is an isomorphism in  $X^* \times Q$ .

**Remark 2.2.8** (Notation). From now on, we will always involve Hilbert spaces. For the sake of notation, there we will denote the various bilinear forms defined by  $A(\boldsymbol{\mu})$ ,  $B(\boldsymbol{\mu})$  and their adjoints ones in the following unique way:

$$\langle A(\boldsymbol{\mu})y, p \rangle_{QQ^*} := a(y, p; \boldsymbol{\mu}) \quad \langle B(\boldsymbol{\mu})u, p \rangle_{QQ^*} := b(u, p; \boldsymbol{\mu}).$$

**2.3. Unsteady Problems.** We briefly recall results on well-posedness for time-dependent Linear-Quadratic OCP( $\boldsymbol{\mu}$ )s based on [50, 51]. We consider saddle-point formulation in order to prove well-posedness by using tools of the previous Sections in the case of null initial conditions. Differently from the steady case, here we will make some more technical assumptions, which will be fulfilled by both ‘‘Graetz-Poiseuille’’ and ‘‘Propagating Front in a Square’’ problems.

Consider two separable Hilbert spaces  $Y$  and  $H$  satisfying  $Y \hookrightarrow H \hookrightarrow Y^*$  and, moreover, other two Hilbert spaces  $U$  and  $Z \supseteq Y$ , where  $Y$  and  $U$  are the usual *state* and *control spaces*, and  $Z$  is the space of observation. We endow them with the standard norms inherited from their respectively scalar products:  $(\cdot, \cdot)_Y$ ,  $(\cdot, \cdot)_Z$ ,  $(\cdot, \cdot)_U$  and  $(\cdot, \cdot)_H$ . We define the following Hilbert spaces:

$$\mathcal{Y} = L^2(0, T; Y), \quad \mathcal{Y}^* = L^2(0, T; Y^*), \quad \mathcal{U} = L^2(0, T; U) \quad \mathcal{Z} := L^2(0, T; Z) \supseteq \mathcal{Y}.$$

with respective norms, for instance in the case of  $\mathcal{Y}$  and  $\mathcal{U}$  given by

$$(9) \quad \|y\|_{\mathcal{Y}}^2 := \int_0^T \|y\|_Y^2 dt, \quad \text{and} \quad \|u\|_{\mathcal{U}}^2 := \int_0^T \|u\|_U^2 dt$$

and similarly for the others. Furthermore, let us define the Hilbert space  $\mathcal{Y}_t$  with its scalar product  $(\cdot, \cdot)_{\mathcal{Y}_t}$ :

$$\mathcal{Y}_t := \left\{ y \in \mathcal{Y} \quad \text{s.t.} \quad \frac{\partial y}{\partial t} \in \mathcal{Y}^* \right\}, \quad (y, z)_{\mathcal{Y}_t} := \int_0^T (y, z)_Y dt + \int_0^T \left( \frac{\partial y}{\partial t}, \frac{\partial z}{\partial t} \right)_{Y^*} dt.$$

Our aim is to solve the following unconstrained Linear-Quadratic *Parametric Parabolic OCP*( $\boldsymbol{\mu}$ ):

**Problem 2.3.1** (Parametric Parabolic OCP( $\boldsymbol{\mu}$ )). For a given  $\boldsymbol{\mu} \in \mathcal{P}$  find the pair  $(y(\boldsymbol{\mu}), u(\boldsymbol{\mu})) \in \mathcal{Y}_t \times \mathcal{U}$  that satisfies

$$(10) \quad \begin{cases} \frac{\partial y(\boldsymbol{\mu})}{\partial t} + A(\boldsymbol{\mu})y(\boldsymbol{\mu}) + B(\boldsymbol{\mu})u(\boldsymbol{\mu}) - f(\boldsymbol{\mu}) = 0, & \text{in } \Omega \times (0, T), \\ \frac{\partial y(\boldsymbol{\mu})}{\partial n} = 0, & \text{on } \Gamma_N \times (0, T), \\ y(\boldsymbol{\mu}) = l, & \text{on } \Gamma_D \times (0, T), \\ y(\boldsymbol{\mu})(0) = y_0, & \text{in } \Omega, \end{cases}$$

and minimizes

$$\min_{(y(\boldsymbol{\mu}), u(\boldsymbol{\mu})) \in \mathcal{Y}_t \times \mathcal{U}} J(y, u; \boldsymbol{\mu}) = \frac{1}{2}m(Oy(\boldsymbol{\mu}) - z_d(\boldsymbol{\mu}), Oy(\boldsymbol{\mu}) - z_d(\boldsymbol{\mu})) + \frac{\alpha}{2}n(u(\boldsymbol{\mu}), u(\boldsymbol{\mu})),$$

where  $m : \mathcal{Y}_t \times \mathcal{Y}_t \rightarrow \mathbb{R}$  and  $n : \mathcal{U} \times \mathcal{U} \rightarrow \mathbb{R}$  are symmetric and continuous bilinear forms,  $z_d(\boldsymbol{\mu}) \in \mathcal{Z}$  is the observed desired solution profile and  $\alpha > 0$  is the fixed penalization parameter. In our test case we will always take  $y_0 \equiv 0$ .

Also in this case, we denote  $y := y(\boldsymbol{\mu})$  and  $u := u(\boldsymbol{\mu})$  omitting the parameter dependence. We can state the weak formulation of (10) as

$$\begin{cases} \int_0^T \left\langle \frac{\partial y}{\partial t}, q \right\rangle_{\mathcal{Y}^* \mathcal{Y}} dt + \int_0^T \langle A(\boldsymbol{\mu})y, q \rangle_{\mathcal{Y}^* \mathcal{Y}} dt + \int_0^T \langle B(\boldsymbol{\mu})u, q \rangle_{\mathcal{Y}^* \mathcal{Y}} dt - \int_0^T \langle f(\boldsymbol{\mu}), q \rangle_{\mathcal{Y}^* \mathcal{Y}} dt = 0, & \forall q \in \mathcal{Y}_t, \\ y(0) = y_0, & \text{in } \Omega, \end{cases}$$

where  $f(\boldsymbol{\mu}) \in \mathcal{Y}^*$  gathers all forcing, boundary and, eventually, lifting terms of the state equation. Nevertheless, for the sake of notation, we will consider  $a : \mathcal{Y}_t \times \mathcal{Y}_t \rightarrow \mathbb{R}$  and  $b : \mathcal{U} \times \mathcal{Y}_t \rightarrow \mathbb{R}$  the bilinear forms defined as  $a(y, q; \boldsymbol{\mu}) = \langle A(\boldsymbol{\mu})y, q \rangle_{\mathcal{Y}^* \mathcal{Y}}$  and  $b(u, q; \boldsymbol{\mu}) = \langle B(\boldsymbol{\mu})u, q \rangle_{\mathcal{Y}^* \mathcal{Y}}$ , respectively. For a proper definition of the adjoint variable, it is opportune to take  $q \in \mathcal{Y}_t$  rather than  $q \in \mathcal{Y}$  [50]. Let us define the state-control product space  $\mathcal{X} = \mathcal{Y}_t \times \mathcal{U}$ . Then we define the operators  $E, D$  and  $\bar{g}$  similarly as made in the steady case in order to make the formulation more compact [50]:

$$(11) \quad \begin{aligned} D(\boldsymbol{\mu}) : \mathcal{X} \times \mathcal{X} &\rightarrow \mathbb{R}, & D(x, \bar{x}, \boldsymbol{\mu}) &= m(Oy, O\bar{y}; \boldsymbol{\mu}) + \alpha n(u, \bar{u}; \boldsymbol{\mu}); \\ E(\boldsymbol{\mu}) : \mathcal{X} \times \mathcal{Y}_t &\rightarrow \mathbb{R}, & E(x, q, \boldsymbol{\mu}) &= \int_0^T \left\langle \frac{\partial y}{\partial t}, q \right\rangle_{\mathcal{Y}^* \mathcal{Y}} dt + \int_0^T a(y, q, \boldsymbol{\mu}) dt + \int_0^T b(u, q, \boldsymbol{\mu}) dt; \\ \bar{g}(\boldsymbol{\mu}) &\in \mathcal{X}^*, & \int_0^T \langle \bar{g}(\boldsymbol{\mu}), \bar{x} \rangle dt &= m(O\bar{y}, z_d(\boldsymbol{\mu})). \end{aligned}$$

Denoting  $p := p(\boldsymbol{\mu})$  and considering  $Q^* = \mathcal{Y}_t$  [50], the Lagrangian and objective functionals are, respectively:

$$(12) \quad \mathcal{L}(x, p; \boldsymbol{\mu}) = J(x; \boldsymbol{\mu}) + E(x, p; \boldsymbol{\mu}) - \int_0^T \langle f(\boldsymbol{\mu}), p \rangle_{\mathcal{Y}^* \mathcal{Y}} dt, \quad J(x, \boldsymbol{\mu}) = \frac{1}{2} D(x, x; \boldsymbol{\mu}) - \int_0^T \langle \bar{g}(\boldsymbol{\mu}), x \rangle dt.$$

As made in the steady case, the minimization of Problem 2.3.1 means to seek the solution of the following system: given  $\boldsymbol{\mu} \in \mathcal{D}$ , find  $(y, u, p) = (x, p) \in \mathcal{X} \times \mathcal{Y}_t$  which solve

$$(13) \quad \begin{cases} \mathcal{L}_y(y, u, p; \boldsymbol{\mu})[\bar{y}] = 0, & \forall \bar{y} \in \mathcal{Y}_t, \\ \mathcal{L}_u(y, u, p; \boldsymbol{\mu})[\bar{u}] = 0, & \forall \bar{u} \in \mathcal{U}, \\ \mathcal{L}_p(y, u, p; \boldsymbol{\mu})[\bar{p}] = 0, & \forall \bar{p} \in \mathcal{Y}_t, \end{cases}$$

and satisfy boundary and initial conditions in Problem 2.3.1 with  $p(T) = 0$  [30]. The saddle-point structure of steady Linear-Quadratic OCP( $\boldsymbol{\mu}$ )s (8) can be derived in the parabolic case, too (here expressed in the weak formulation) [50]:

$$(14) \quad \begin{cases} D(x, w; \boldsymbol{\mu}) + E(w, p; \boldsymbol{\mu}) = \int_0^T \langle \bar{g}(\boldsymbol{\mu}), w \rangle dt, & \forall w \in \mathcal{X}, \\ E(x, q; \boldsymbol{\mu}) = \int_0^T \langle f(\boldsymbol{\mu}), q \rangle_{\mathcal{Y}^* \mathcal{Y}} dt, & \forall q \in \mathcal{Y}_t. \end{cases}$$

The equivalence between the optimality system and saddle-point formulation for Linear-Quadratic Parabolic OCP( $\boldsymbol{\mu}$ )s is straightforward. For well-posedness the following assumption is needed [50].

**Assumption 2.3.2.** *The bilinear forms  $n(\cdot, \cdot; \boldsymbol{\mu})$ ,  $m(\cdot, \cdot; \boldsymbol{\mu})$ ,  $b(\cdot, \cdot; \boldsymbol{\mu})$ , and  $a(\cdot, \cdot; \boldsymbol{\mu})$  satisfy the following features:*

- (1)  $m(\cdot, \cdot; \boldsymbol{\mu})$  is positive definite, continuous, and symmetric.
- (2)  $n(\cdot, \cdot; \boldsymbol{\mu})$  is coercive, continuous, and symmetric;
- (3) there exists  $C_a > 0$  s.t.  $a(w, w; \boldsymbol{\mu}) \geq C_a(\boldsymbol{\mu}) \|w\|_{\mathcal{Y}}^2$ ,  $\forall w \in \mathcal{Y}_t$ ;
- (4) there exists  $c_a > 0$  s.t.  $|a(w, p; \boldsymbol{\mu})| \leq c_a(\boldsymbol{\mu}) \|w\|_{\mathcal{Y}} \|p\|_{\mathcal{Y}}$ ,  $\forall w, p \in \mathcal{Y}_t$ ;

(5) there exists  $c_b > 0$  s.t.  $|b(v, p; \boldsymbol{\mu})| \leq c_b(\boldsymbol{\mu}) \|v\|_U \|p\|_Y$ ,  $\forall v \in \mathcal{U}$  and  $\forall p \in \mathcal{Y}_t$ ;

Finally, one can prove the well-posedness of Problem 2.3.1 (for more details, we refer to [50]).

**Theorem 2.3.3** (Well-posedness of Parabolic OCP( $\boldsymbol{\mu}$ )s). [50] *Under Assumption 2.3.2 the saddle-point formulation (14) satisfies the hypothesis (1) of Theorem 2.2.7, hence the solution is unique.*

**Assumption 2.3.4.** *For both steady and unsteady problems, we will consider the Identity operator restricted to our observation domain  $\Omega_{obs}$  as the Observation function  $O$ . Therefore,  $\mathcal{Z} = \mathcal{Y}$  is assumed and our desired state will be denoted by  $y_d$ .*

### 3. TRUTH DISCRETIZATION

In this Section we firstly pursue a numerical method for the solution of an OCP: a discretization of the optimality system (6) will be given following an *one shot* or *all-at-once approach* [23, 46, 47]. Secondly, we will consider SUPG stabilization for Advection-Dominated equations in case of high Péclet number. An *optimize-then-discretize* approach is followed, i.e. at first we derive optimality conditions as system (6) and then we discretize it. Therefore, we obtain a discretized system:

$$(15) \quad \begin{cases} \mathcal{L}_{y^{\mathcal{N}}}(y^{\mathcal{N}}, u^{\mathcal{N}}, p^{\mathcal{N}}) = J_{y^{\mathcal{N}}}(y^{\mathcal{N}}, u^{\mathcal{N}}) + e_{y^{\mathcal{N}}}(y^{\mathcal{N}}, u^{\mathcal{N}})^* p^{\mathcal{N}} = 0 & \text{in } (Y^{\mathcal{N}})^* \\ \mathcal{L}_{u^{\mathcal{N}}}(y^{\mathcal{N}}, u^{\mathcal{N}}, p^{\mathcal{N}}) = J_{u^{\mathcal{N}}}(y^{\mathcal{N}}, u^{\mathcal{N}}) + e_{u^{\mathcal{N}}}(y^{\mathcal{N}}, u^{\mathcal{N}})^* p^{\mathcal{N}} = 0 & \text{in } (U^{\mathcal{N}})^* \\ \mathcal{L}_{p^{\mathcal{N}}}(y^{\mathcal{N}}, u^{\mathcal{N}}, p^{\mathcal{N}}) = e(y^{\mathcal{N}}, u^{\mathcal{N}}) = 0 & \text{in } Q^{\mathcal{N}}, \end{cases}$$

where  $\mathcal{L}_{y^{\mathcal{N}}}, \mathcal{L}_{u^{\mathcal{N}}}, \mathcal{L}_{p^{\mathcal{N}}}$  are the discretizations of partial derivatives of  $\mathcal{L}$  and  $Y^{\mathcal{N}}, U^{\mathcal{N}}, Q^{\mathcal{N}}$  are the approximation of  $Y, U, Q$ , respectively.

Let us start our discussion from the steady case. From now on we will always assume to work with  $Y, U, Q$  Hilbert spaces. We employ a FEM discretization, which will be named as the *high-fidelity* or *truth* approximation. We consider  $\Omega_h$  as a quasi-uniform mesh on the domain  $\Omega$ , for which the parameter  $h$  indicates the *mesh size*, i.e. maximum diameter of an element of the grid.  $\mathcal{T}_h$  is a regular triangularization on  $\Omega$  and

$$\Omega_h := \text{int} \left( \bigcup_{K \in \mathcal{T}_h} K \right),$$

where  $K$  is a triangle of  $\mathcal{T}_h$ . We define the FEM spaces  $Y^{\mathcal{N}} = Y \cap X^{\mathcal{N},r}$ ,  $U^{\mathcal{N}} = U \cap X^{\mathcal{N},r}$  and  $(Q^{\mathcal{N}})^* = Q^* \cap X^{\mathcal{N},r}$ , where

$$X^{\mathcal{N},r} = \left\{ v^{\mathcal{N}} \in C^0(\bar{\Omega}) : v|_K \in \mathbb{P}^r(K), \forall K \in \mathcal{T}_h \right\}$$

and  $\mathbb{P}^r(K)$  represents the space of polynomials of degree at most equal to  $r$  defined on a triangle  $K$ . As we will remark later, we will always use the same triangulation  $\mathcal{T}_h$  and a  $\mathbb{P}^1$ -FEM approximation for state, control and adjoint variables. The dimensions of  $Y^{\mathcal{N}}, U^{\mathcal{N}}, Q^{\mathcal{N}}$  are all equal to  $\mathcal{N}$ . The overall dimension of the discrete problem is  $\mathcal{N}_{tot} = 3 \cdot \mathcal{N}$ . For the sake of simplicity, we assume  $Q_h^* = Y^{\mathcal{N}}$ . Moreover, we indicate with  $X^{\mathcal{N}} = Y^{\mathcal{N}} \times U^{\mathcal{N}} \subset X$ . From now on we will refer to the same symbol  $y_d$  to also indicate the FEM discretization version of the desired state.

The discretization of a Linear-Quadratic OCP of Problem 2.1.1 reads as

$$\min_{(y^{\mathcal{N}}, u^{\mathcal{N}}) \in Y^{\mathcal{N}} \times U^{\mathcal{N}}} J(y^{\mathcal{N}}, u^{\mathcal{N}}) = \frac{1}{2} m(y^{\mathcal{N}} - y_d, y^{\mathcal{N}} - y_d) + \frac{\alpha}{2} n(u^{\mathcal{N}}, u^{\mathcal{N}}) \text{ s.t. } e(y^{\mathcal{N}}, u^{\mathcal{N}}) = 0.$$

Moreover, the operators  $m$  and  $n$  will be the  $L^2$  product on  $\Omega_{obs}$  and on  $\Omega$ , respectively.

For the saddle-point system, we define the operators  $\bar{g}^{\mathcal{N}} : X^{\mathcal{N}} \rightarrow \mathbb{R}$ ,  $f^{\mathcal{N}} : Y^{\mathcal{N}} \rightarrow \mathbb{R}$ ,  $D^{\mathcal{N}} : X^{\mathcal{N}} \rightarrow (X^{\mathcal{N}})^*$ , and  $E^{\mathcal{N}} : X^{\mathcal{N}} \rightarrow (Q^{\mathcal{N}})^*$  as just the usual restrictions

$$(16) \quad \begin{aligned} \langle \bar{g}^{\mathcal{N}}, \bar{x}^{\mathcal{N}} \rangle_{(X^{\mathcal{N}})^* X^{\mathcal{N}}} &= \langle \bar{g}, \bar{x} \rangle_{X^* X}, & \langle D^{\mathcal{N}} x^{\mathcal{N}}, \bar{x}^{\mathcal{N}} \rangle_{(X^{\mathcal{N}})^* X^{\mathcal{N}}} &= \langle D x^{\mathcal{N}}, \bar{x}^{\mathcal{N}} \rangle_{X^* X}, \\ \langle f^{\mathcal{N}}, \bar{p}^{\mathcal{N}} \rangle_{(Y^{\mathcal{N}})^* Y^{\mathcal{N}}} &= \langle f, \bar{p} \rangle_{Q^* Q^*}, & \langle E^{\mathcal{N}} x^{\mathcal{N}}, \bar{p}^{\mathcal{N}} \rangle_{(Y^{\mathcal{N}})^* Y^{\mathcal{N}}} &= \langle E x^{\mathcal{N}}, \bar{p}^{\mathcal{N}} \rangle_{Q^* Q^*}, \end{aligned}$$

for all  $x^{\mathcal{N}} \in X^{\mathcal{N}}, \bar{p}^{\mathcal{N}} \in Y^{\mathcal{N}}$ .

We highlight the algebraic structure of the discretize optimality system. We define the basis of the finite spaces  $X^{\mathcal{N}}$  and  $Y^{\mathcal{N}}$  as below:

$$(17) \quad \{\varphi_j \in X^{\mathcal{N}}\}_{j=1}^{2\mathcal{N}}, \quad \{\psi_k \in Y^{\mathcal{N}}\}_{k=1}^{\mathcal{N}}.$$

As a result, we can rewrite a pair  $(x^{\mathcal{N}}, p^{\mathcal{N}}) \in X^{\mathcal{N}} \times Y^{\mathcal{N}}$  in the following way:

$$\left( x^{\mathcal{N}} = \sum_{j=1}^{2\mathcal{N}} x_j \varphi_j, \quad p^{\mathcal{N}} = \sum_{k=1}^{\mathcal{N}} p_k \psi_k \right).$$

Therefore, we can define  $\mathcal{D} \in \mathbb{R}^{2\mathcal{N} \times 2\mathcal{N}}$ ,  $\mathcal{E} \in \mathbb{R}^{\mathcal{N} \times 2\mathcal{N}}$ ,  $\bar{\mathbf{g}} \in \mathbb{R}^{2\mathcal{N}}$  and  $\mathbf{f} \in \mathbb{R}^{\mathcal{N}}$  as follows:

$$(18) \quad \begin{aligned} \mathcal{D}_{ij} &= \langle D^{\mathcal{N}} \varphi_i, \varphi_j \rangle_{(X^{\mathcal{N}})^* X^{\mathcal{N}}}, & \mathcal{E}_{lm} &= \langle E^{\mathcal{N}} \varphi_l, \psi_m \rangle_{(Y^{\mathcal{N}})^* Y^{\mathcal{N}}}, \\ \bar{\mathbf{g}}_k &= \langle \bar{g}^{\mathcal{N}}, \varphi_k \rangle_{(X^{\mathcal{N}})^* X^{\mathcal{N}}}, & \mathbf{f}_n &= \langle f^{\mathcal{N}}, \psi_n \rangle_{(Y^{\mathcal{N}})^* Y^{\mathcal{N}}}. \end{aligned}$$

Finally, we can build the following saddle point system, with a block structure:

$$(19) \quad \begin{pmatrix} \mathcal{D} & \mathcal{E}^T \\ \mathcal{E} & 0 \end{pmatrix} \begin{pmatrix} \mathbf{x} \\ \mathbf{p} \end{pmatrix} = \begin{pmatrix} \bar{\mathbf{g}} \\ \mathbf{f} \end{pmatrix},$$

where  $(\mathbf{x})_i = x_i, i = 1, \dots, 2\mathcal{N}$  and  $(\mathbf{p})_k = p_k, k = 1, \dots, \mathcal{N}$ . For this purpose, let us denote with  $\mathbf{y}$ ,  $\mathbf{u}$  and  $\mathbf{p}$  the vectors of coefficients of  $y^{\mathcal{N}}$ ,  $u^{\mathcal{N}}$  and  $p^{\mathcal{N}}$ , expressed in terms of the nodal basis (17) by splitting components of  $X^{\mathcal{N}}$  in those of  $Y^{\mathcal{N}}$  and  $U^{\mathcal{N}}$ . We express with  $\mathbf{y}_d$  the vector with the components of the discretized desired state, i.e. the Galerkin projection of  $y_d$  on  $Y^{\mathcal{N}}$ . Moreover, let us indicate the stiffness matrix derived from the bilinear form  $a(\cdot, \cdot)$  with  $K$ ,  $K^T$  is the stiffness matrix related to  $a^*$  and the mass matrix is denoted with  $M$ . In addition, we call  $B$ ,  $B^T$  is the mass matrix related to the forms  $b$  and  $b^*$ . We have that:

$$\mathcal{D} = \begin{pmatrix} M & 0 \\ 0 & \alpha M \end{pmatrix}, \quad \mathcal{E} = \begin{pmatrix} K & B \end{pmatrix}, \quad \mathbf{x} = \begin{pmatrix} \mathbf{y} \\ \mathbf{u} \end{pmatrix}, \quad \bar{\mathbf{g}} = \begin{pmatrix} M \mathbf{y}_d \\ 0 \end{pmatrix}.$$

and the optimality system shows this block structure:

$$(20) \quad \begin{pmatrix} M & 0 & K^T \\ 0 & \alpha M & B^T \\ K & B & 0 \end{pmatrix} \begin{pmatrix} \mathbf{y} \\ \mathbf{u} \\ \mathbf{p} \end{pmatrix} = \begin{pmatrix} M \mathbf{y}_d \\ 0 \\ \mathbf{f} \end{pmatrix}.$$

**3.1. SUPG stabilization for Advection-Dominated OCP( $\mu$ )s.** In this Section we illustrate Advection-Dominated OCP( $\mu$ )s and the SUPG technique applied to an *optimize-then-discretize* approach. From now, we recall the dependence on parameters of our operators. Let us start from our definition of an *Advection-Diffusion equation*.

**Definition 3.1.1** (Advection-Diffusion Equations). *Let us consider the following problem:*

$$(21) \quad L(\mu)y := -\varepsilon(\mu)\Delta y + \mathbf{b}(\mu) \cdot \nabla y = f(\mu) \text{ in } \Omega \subset \mathbb{R}^2,$$

with suitable boundary conditions on  $\partial\Omega$ . Let us suppose that:

- the diffusion coefficient  $\varepsilon : \Omega \rightarrow \mathbb{R}$  belongs to  $L^\infty(\Omega)$  and depends on the parameter  $\mu$ . We assume there exists a constant  $\bar{\varepsilon} > 0$  such that  $\varepsilon(x) \geq \bar{\varepsilon}, \forall x \in \Omega$ ;
- the advection field  $\mathbf{b} : \Omega \rightarrow \mathbb{R}^2$  belongs to  $(L^\infty(\Omega))^2$  and depends on the parameter  $\mu$ . We suppose that  $0 \geq \operatorname{div} \mathbf{b}(x) \geq -\tilde{k}$ , holds for all  $x \in \Omega$ , with  $\tilde{k} \in \mathbb{R}_0^+$ ;
- $f(\mu) : \Omega \rightarrow \mathbb{R}$  is an  $L^2(\Omega)$ -function that can depend on the parameter  $\mu$ .

In this case, (21) is an Advection-Diffusion problem and the operator  $L(\mu)y := -\varepsilon(\mu)\Delta y + \mathbf{b}(\mu) \cdot \nabla y$  is said the Advection-Diffusion operator.

From (21), we can easily derive the weak formulation of an Advection-Diffusion problem:

$$(22) \quad \text{find } y \in Y \text{ s.t. } a(y, q; \mu) = F(q; \mu) \quad \forall q \in Q^*,$$



where

$$(23) \quad a(y, q; \boldsymbol{\mu}) := \int_{\Omega} \varepsilon(\boldsymbol{\mu}) \nabla y \nabla q + \mathbf{b}(\boldsymbol{\mu}) \cdot \nabla y q \, dx, \quad F(q; \boldsymbol{\mu}) := \int_{\Omega} f(\boldsymbol{\mu}) q \, dx, \quad y \in Y, q \in Q^*.$$

From a numerical point of view, when the advection term  $\mathbf{b}(\boldsymbol{\mu}) \cdot \nabla u$  “dominates” the diffusive one  $-\varepsilon(\boldsymbol{\mu}) \Delta u$ , i.e. when  $|\mathbf{b}(\boldsymbol{\mu})| \gg \varepsilon(\boldsymbol{\mu})$ , the approximated solution can show instability phenomena along the direction of the advection field [42]. In order to give an indicator of the instability, let us consider the regular triangulation  $\mathcal{T}_h$  related to FEM discretization. For any element  $K \in \mathcal{T}_h$ , we can then define the *local Péclet number* as [42, 38]:

$$(24) \quad \mathbb{P}e_K(x) := \frac{|\mathbf{b}(x)| h_K}{2\varepsilon(x)}, \quad \forall x \in K,$$

where  $h_K$  is the diameter of  $K$ .

**Definition 3.1.2** (Advection-Dominated problem). *Considering Definition 3.1.1 we are dealing with an Advection-Dominated problem if  $\mathbb{P}e_K(x) > 1$ ,  $\forall x \in K$ ,  $\forall K \in \mathcal{T}_h$ .*

To solve the issue of the instability, we will exploit the SUPG method [11, 25, 26, 42], which is a *strongly consistent stabilization technique*; i.e. is consistent for weak PDEs and its order of accuracy can be greater than one. Let us now consider the Advection-Diffusion operator (21): for the sake of simplicity, we define it on  $H_0^1(\Omega)$  and we do not indicate the parameter dependence. The operator  $L$  can be split into its symmetric and skew-symmetric parts [42], defined as:

$$(25) \quad \begin{aligned} \text{symmetric part: } L_S y &= -\varepsilon \Delta y - \frac{1}{2} (\operatorname{div} \mathbf{b}) y, \quad \forall y \in H_0^1(\Omega), \\ \text{skew-symmetric part: } L_{SS} y &= \mathbf{b} \cdot \nabla y + \frac{1}{2} (\operatorname{div} \mathbf{b}) y, \quad \forall y \in H_0^1(\Omega), \end{aligned}$$

i.e.  $L = L_S + L_{SS}$ . Symmetric and skew-symmetric parts can be directly derived using the formulae:

$$(26) \quad L_S = \frac{L + L^*}{2}, \quad L_{SS} = \frac{L - L^*}{2},$$

where  $L^*$  is the adjoint operator related to  $L$ .

Now, let us analyze our OCP problem (6): we follow the *optimize-then-discretize* approach in [14]. The *discretized state equation* is described as follows, where the control is distributed, i.e. it acts on the whole domain  $\Omega$ :

$$(27) \quad a_s(y^{\mathcal{N}}, q^{\mathcal{N}}) + b_s(u^{\mathcal{N}}, q^{\mathcal{N}}) = F_s(q^{\mathcal{N}}), \quad \forall q^{\mathcal{N}} \in (Q^{\mathcal{N}})^*,$$

with

$$(28) \quad a_s(y^{\mathcal{N}}, q^{\mathcal{N}}) := a(y^{\mathcal{N}}, q^{\mathcal{N}}) + \sum_{K \in \mathcal{T}_h} \delta_K \left( L y^{\mathcal{N}}, \frac{h_K}{|\mathbf{b}|} L_{SS} q^{\mathcal{N}} \right)_K,$$

$$(29) \quad b_s(u^{\mathcal{N}}, q^{\mathcal{N}}) := - \int_{\Omega} u^{\mathcal{N}} q^{\mathcal{N}} - \sum_{K \in \mathcal{T}_h} \delta_K \left( u^{\mathcal{N}}, \frac{h_K}{|\mathbf{b}|} L_{SS} q^{\mathcal{N}} \right)_K,$$

and

$$(30) \quad F_s(q^{\mathcal{N}}) := F(q^{\mathcal{N}}) + \sum_{K \in \mathcal{T}_h} \delta_K \left( f, \frac{h_K}{|\mathbf{b}|} L_{SS} q^{\mathcal{N}} \right)_K,$$

where  $(\cdot, \cdot)_K$  indicates the usual  $L^2(K)$ -product,  $f$  collects all the forcing and lifting terms, and  $\delta_K$  denotes a positive dimensionless stabilization parameter related to an element  $K \in \mathcal{T}_h$ . In principle, since  $\delta_K$  is local, it can be different for each  $K$ . Considering the adjoint equation, we can see that it is also an Advection-Dominated equation, but with an advective term with opposite sign with respect to the state one. As a matter of fact, from (26) we obtain that  $L^* = L_S - L_{SS}$ . The SUPG method leads to the *discretized adjoint equation*

$$(31) \quad a_s^*(z^{\mathcal{N}}, p^{\mathcal{N}}) + (y^{\mathcal{N}} - y_d, z^{\mathcal{N}})_s = 0, \quad \forall z^{\mathcal{N}} \in Y^{\mathcal{N}},$$

with

$$(32) \quad \begin{aligned} a_s^*(z^\mathcal{N}, p^\mathcal{N}) &:= a^*(z^\mathcal{N}, p^\mathcal{N}) + \sum_{K \in \mathcal{T}_h} \delta_K^a \left( (L_S - L_{SS})p^\mathcal{N}, \frac{h_K}{|\mathbf{b}|} (-L_{SS})z^\mathcal{N} \right)_K, \\ (y^\mathcal{N} - y_d, z^\mathcal{N})_s &:= \int_{\Omega_{obs}} (y^\mathcal{N} - y_d)z^\mathcal{N} \, dx + \sum_{K \in \mathcal{T}_h|_{\Omega_{obs}}} \delta_K^a \left( y^\mathcal{N} - y_d, \frac{h_K}{|\mathbf{b}|} (-L_{SS})z^\mathcal{N} \right)_K, \end{aligned}$$

where  $a^*$  is the adjoint form of  $a$  and  $\delta_K^a$  is the parameter related to the stabilized adjoint bilinear forms. As in this work we consider  $\delta_K = \delta_K^a$  in numerical simulations, from now on we will always denote both stabilization parameter with  $\delta_K$ . Instead, the *discretized gradient equation* is not affected by the SUPG and it remains untouched:

$$(33) \quad b^*(v^\mathcal{N}, p^\mathcal{N}) + \alpha n(u^\mathcal{N}, v^\mathcal{N}) = 0, \quad \forall v^\mathcal{N} \in U^\mathcal{N}.$$

With this setting it follows a nonsymmetric system for the computation of the numerical solution, but we gain the strongly-consistency of the method for the optimality system if  $y, u, p$  are regular [14]. To summarize, the SUPG optimality system for a steady OCP is the following:

$$(34) \quad \begin{aligned} \text{discretized adjoint equation:} & \quad a_s^*(z^\mathcal{N}, p^\mathcal{N}) + (y^\mathcal{N} - y_d, z^\mathcal{N})_s = 0, \quad \forall z^\mathcal{N} \in Y^\mathcal{N}, \\ \text{discretized gradient equation:} & \quad b^*(v^\mathcal{N}, p^\mathcal{N}) + \alpha n(u^\mathcal{N}, v^\mathcal{N}) = 0, \quad \forall v^\mathcal{N} \in U^\mathcal{N}, \\ \text{discretized state equation:} & \quad a_s(y^\mathcal{N}, q^\mathcal{N}) + b_s(u^\mathcal{N}, q^\mathcal{N}) = F_s(q^\mathcal{N}), \quad \forall q^\mathcal{N} \in (Q^\mathcal{N})^*, \end{aligned}$$

and, referring to (20), the discretized algebraic system reads as:

$$(35) \quad \begin{pmatrix} M_s & 0 & K_s^T \\ 0 & \alpha M & B^T \\ K_s & B_s & 0 \end{pmatrix} \begin{pmatrix} \mathbf{y} \\ \mathbf{u} \\ \mathbf{p} \end{pmatrix} = \begin{pmatrix} M_s \mathbf{y}_d \\ 0 \\ \mathbf{f}_s \end{pmatrix},$$

where  $M_s$  is the stabilized mass matrix related to  $m$ ,  $M$  is the not-stabilized mass matrix related to  $n$ ,  $K_s$  and  $K_s^T$  are the stiffness matrices related to  $a_s$  and  $a_s^*$ , respectively,  $B_s$  is the stabilized mass matrix related to  $b_s$ ,  $B^T$  is the block linked to  $b^*$  and  $f_s$  is the vector whose components are the coefficients of the stabilized force term. Every block is derived as in (18).

We indicate with  $||| \cdot |||$  the energy norm related to the bilinear form  $a$  belonging to Advection-Diffusion equations (3.1.1), i.e.

$$(36) \quad |||w|||^2 := \varepsilon \|\nabla w\|_{L^2(\Omega)}^2 + \frac{1}{2} \left\| (\operatorname{div} \mathbf{b})^{\frac{1}{2}} w \right\|_{L^2(\Omega)}^2, \quad \forall w \in H_0^1(\Omega).$$

Therefore, we define the SUPG norm on  $H_0^1(\Omega)$  as

$$(37) \quad \|w\|_{SUPG}^2 := |||w|||^2 + \sum_{K \in \mathcal{T}_h} \delta_K \left( L_{SS} w, \frac{h_K}{|\mathbf{b}|} L_{SS} w \right)_K, \quad \forall w \in H_0^1(\Omega).$$

Considering that (38) holds true, it is immediate to see that the SUPG bilinear form (28) is coercive with respect to the SUPG norm [42]. Finally, we can illustrate an estimate of the error for the adjoint and the state variables of the solution of an OCP [14].

**Theorem 3.1.3** (Error for state and adjoint variables). *Let  $m, r \geq 1$  and  $(y, u, p)$  be the solution of (6) with  $y \in H^{m+1}(\Omega), p \in H^{r+1}(\Omega)$ . Furthermore, let  $y^\mathcal{N}, u^\mathcal{N}, p^\mathcal{N}$  be the numerical solution of (34). If  $\delta_K$  satisfies*

$$(38) \quad 0 < \delta_K \leq \frac{h_K}{\varepsilon \eta_{inv}^2} \quad \text{and} \quad \delta_K = \begin{cases} \delta_1 \frac{h_K}{\varepsilon}, & \text{Pe}_K(x) \leq 1, \\ \delta_2, & \text{Pe}_K(x) > 1, \end{cases}$$

where  $\delta_1, \delta_2 > 0$  are chosen constant, and  $\eta_{inv}$  is defined as the following inverse constant

$$|y^\mathcal{N}|_{1,K} \leq \eta_{inv} h_K^{-1} \|y^\mathcal{N}\|_{L^2(K)} \quad \text{and} \quad \|\Delta y^\mathcal{N}\|_{L^2(K)} \leq \eta_{inv} h_K^{-1} \|\nabla y^\mathcal{N}\|_{L^2(K)} \quad \forall y^\mathcal{N} \in Y^\mathcal{N},$$

with  $|\cdot|_{1,K}$ ,  $\|\cdot\|_K$  seminorm and  $L^2$ -norm on  $K$ , respectively, then there exists  $C > 0$  such that

$$(39) \quad \begin{aligned} \|y - y^{\mathcal{N}}\|_{SUPG} &\leq C \left( h^m \left( \varepsilon^{1/2} + h^{1/2} \right) |y|_{H^{m+1}(\Omega)} + \|u^{\mathcal{N}} - u\|_{L^2(\Omega)} \right), \quad \forall h, \\ \|p - p^{\mathcal{N}}\|_{SUPG} &\leq C \left( h^r \left( \varepsilon^{1/2} + h^{1/2} \right) |p|_{H^{r+1}(\Omega)} + \|y^{\mathcal{N}} - y\|_{L^2(\Omega)} \right), \quad \forall h. \end{aligned}$$

**3.2. SUPG for Time-Dependent Advection-Dominated OCP( $\mu$ )s.** We briefly discuss the SUPG technique employed with time-dependent problems. Referring to (13), the main challenge comes from the fact that the time derivative should also enter into stabilization framework to ensure consistency [27]. However, other approaches have been proposed: in [45], for instance, the time-derivative is not stabilized. Nevertheless, our discussion follows works inherent to Graetz-Poiseuille and Propagating Front in a Square problems without optimal control [37, 54], where stabilization is used for time derivative, too. This adds nonsymmetric terms to the discretized state and adjoint equations for time derivatives. To the best of our knowledge SUPG for Parabolic OCPs in an *optimize-then-discretized* approach is still a novelty element in literature from a theoretical point of view. However, we refer to [17, 20, 27] for SUPG applied to general Parabolic equations.

We firstly discretize the equation in time, considering each discrete time as a steady-state Advection-Diffusion equation, in a *space-time* approach, and then stabilized it with the SUPG. The time interval  $(0, T)$  is divided in  $N_t$  sub-intervals of equal length  $\Delta t := t_i - t_{i-1}$ ,  $i \in \{1, \dots, N_t\}$ . On the other hand, all terms involving time-derivative go through a time discretization equivalent to a classical implicit Euler approach [3, 23, 46, 50, 51, 52]. The backward Euler method is used to discretize the state equation forward in time, instead the adjoint equation is discretized backward in time using the forward Euler method, which is equivalent to the backward Euler with respect to time  $T - t$ , for  $t \in (0, T)$  [16, 50]. The global dimension of the discrete spaces is  $\mathcal{N}_{tot} = 3 \cdot \mathcal{N} \cdot N_t$ . We recall that  $Y, U, Q$  are Hilbert Spaces and that  $Y^{\mathcal{N}} \equiv (Q^{\mathcal{N}})^*$ .

For the state equation, the stabilized term added to the form related to the time derivative of the state  $\frac{\partial y}{\partial t}$  and the bilinear form  $a$  is the following [27, 37, 54]:

$$s(y^{\mathcal{N}}(t), q^{\mathcal{N}}) = \sum_{K \in \mathcal{T}_h} \delta_K \left( \frac{\partial y^{\mathcal{N}}(t)}{\partial t} + (L_S + L_{SS})y^{\mathcal{N}}(t), \frac{h_K}{|\mathbf{b}|} L_{SS} q^{\mathcal{N}} \right)_K,$$

where  $y^{\mathcal{N}}(t) \in Y^{\mathcal{N}}$  for each  $t \in (0, T)$  and  $q^{\mathcal{N}} \in Y^{\mathcal{N}}$ . Instead, the stabilized term added to the form related to the time derivative of the adjoint  $\frac{\partial p}{\partial t}$  and the bilinear form  $a^*$  is:

$$s^*(z^{\mathcal{N}}, p^{\mathcal{N}}(t)) = \sum_{K \in \mathcal{T}_h} \delta_K \left( -\frac{\partial p^{\mathcal{N}}(t)}{\partial t} + (L_S - L_{SS})p^{\mathcal{N}}(t), -\frac{h_K}{|\mathbf{b}|} L_{SS} z^{\mathcal{N}} \right)_K.$$

We can write the discretized state formulation using a backward Euler approach as follows:

$$(40) \quad \begin{aligned} &\text{for each } i \in \{1, 2, \dots, N_t\}, \text{ find } y_i^{\mathcal{N}} \in Y^{\mathcal{N}} \text{ s.t. } \forall q^{\mathcal{N}} \in Y^{\mathcal{N}}, \\ &\frac{1}{\Delta t} m_s(y_i^{\mathcal{N}}(\boldsymbol{\mu}) - y_{i-1}^{\mathcal{N}}(\boldsymbol{\mu}), q^{\mathcal{N}}; \boldsymbol{\mu}) + a_s(y_i^{\mathcal{N}}(\boldsymbol{\mu}), q^{\mathcal{N}}; \boldsymbol{\mu}) + b_s(u_i^{\mathcal{N}}, q^{\mathcal{N}}; \boldsymbol{\mu}) = F_s(q^{\mathcal{N}}; \boldsymbol{\mu}), \end{aligned}$$

given the initial condition  $y_0^{\mathcal{N}}$  which satisfies

$$(41) \quad (y_0^{\mathcal{N}}, q^{\mathcal{N}})_{L^2(\Omega)} = (y_0, q^{\mathcal{N}})_{L^2(\Omega)}, \quad \forall q^{\mathcal{N}} \in Y^{\mathcal{N}}.$$

The stabilized term  $m_s$  above is defined as:

$$(42) \quad m_s(y^{\mathcal{N}}, q^{\mathcal{N}}; \boldsymbol{\mu}) = (y^{\mathcal{N}}, q^{\mathcal{N}})_{L^2(\Omega)} + \sum_{K \in \mathcal{T}_h} \delta_K \left( y^{\mathcal{N}}, \frac{h_K}{|\mathbf{b}|} L_{SS} q^{\mathcal{N}} \right)_K$$

and it is related to the time discretization; instead,  $a_s$  and  $F_s$  are defined as in the steady case. Similarly we can derive the same for the adjoint forms applying a forward Euler method:

$$(43) \quad \begin{aligned} &\text{for each } i \in \{N_t - 1, N_t - 2, \dots, 1\}, \text{ find } p_i^{\mathcal{N}} \in Y^{\mathcal{N}} \text{ s.t.} \\ &\frac{1}{\Delta t} m_s^*(p_i^{\mathcal{N}}(\boldsymbol{\mu}) - p_{i+1}^{\mathcal{N}}(\boldsymbol{\mu}), z^{\mathcal{N}}; \boldsymbol{\mu}) + a_s^*(z^{\mathcal{N}}, p_i^{\mathcal{N}}(\boldsymbol{\mu}); \boldsymbol{\mu}) = -(y_i^{\mathcal{N}} - y_{d_i}, z^{\mathcal{N}})_s \quad \forall z^{\mathcal{N}} \in Y^{\mathcal{N}}. \end{aligned}$$

The stabilized term  $m_s^*$  above is defined as:

$$(44) \quad m_s^*(p^\mathcal{N}, z^\mathcal{N}; \boldsymbol{\mu}) = (p^\mathcal{N}, z^\mathcal{N})_{L^2(\Omega)} - \sum_{K \in \mathcal{T}_h} \delta_K \left( p^\mathcal{N}, \frac{h_K}{|\mathbf{b}|} L_{SS} z^\mathcal{N} \right)_K.$$

Now we give a look at the discretization scheme. As in the steady case,  $y_i \in Y^\mathcal{N}$ ,  $u_i \in U^\mathcal{N}$  and  $p_i \in Y^\mathcal{N}$ , for  $1 \leq i \leq N_t$ , represent the column vectors including the coefficients of the FEM discretization for state, control and adjoint, respectively. Therefore, we define  $\mathbf{y} = [y_1^T, \dots, y_{N_t}^T]^T$ ,  $\mathbf{u} = [u_1^T, \dots, u_{N_t}^T]^T$  and  $\mathbf{p} = [p_1^T, \dots, p_{N_t}^T]^T$ . The vector  $\mathbf{f}_s = [f_{s_1}^T, \dots, f_{s_{N_t}}^T]^T$  indicates the components of the stabilized forcing term,  $\mathbf{y}_d = [y_{d_1}^T, \dots, y_{d_{N_t}}^T]^T$  is the vector made of discrete time components of our desired state solution; instead,  $\mathbf{y}_0 = [y_0^T, 0^T, \dots, 0^T]^T$  indicates the vector of initial condition for the state, where 0 is the zero vector in  $\mathbb{R}^\mathcal{N}$ . The block matrix system is described as follows.

- *State equation.* We recall that  $K_s$  and  $B_s$  are the matrices associated to the stabilized bilinear forms  $a_s$  and  $b_s$ . Using the backward Euler along time, one has to solve

$$(45) \quad M_s y_i + \Delta t K_s y_i + \Delta t B_s u_i = M_s y_{i-1} + f_{s_i} \Delta t \quad \text{for } i \in \{1, 2, \dots, N_t\},$$

where  $M_s$  is the stabilized mass matrix relative to the FEM discretization of  $m_s$ . Therefore the related block matrix subsystem is

$$\underbrace{\begin{bmatrix} M_s + \Delta t K_s & 0 & & & \\ -M_s & M_s + \Delta t K_s & & & \\ & \ddots & \ddots & & \\ & & 0 & -M_s & M_s + \Delta t K_s \end{bmatrix}}_{\mathcal{A}_s} \mathbf{y} + \Delta t \underbrace{\begin{bmatrix} B_s & 0 \\ 0 & \ddots & 0 \\ 0 & & B_s \end{bmatrix}}_{\mathcal{C}_s} \mathbf{u} = \mathcal{M}_s \mathbf{y}_0 + \Delta t \mathbf{f}_s,$$

where  $\mathcal{M}_s$  is a block diagonal matrix in  $\mathbb{R}^{\mathcal{N} \cdot N_t} \times \mathbb{R}^{\mathcal{N} \cdot N_t}$  whose element on the main diagonal are  $[M_s, \dots, M_s]$ . Then everything can be recast in a more compact form as

$$(46) \quad \mathcal{A}_s \mathbf{y} + \Delta t \mathcal{C}_s \mathbf{u} = \mathcal{M}_s \mathbf{y}_0 + \Delta t \mathbf{f}_s.$$

- *Gradient equation.* We recall that  $B^T$  indicates the mass matrix related to the  $b^*$  form and hence at every time step we have to solve the equation

$$(47) \quad \alpha \Delta t M u_i + \Delta t B^T p_i = 0, \quad \forall i \in \{1, 2, \dots, N_t\},$$

which translates into the following block system:

$$\Delta t \cdot \alpha \underbrace{\begin{bmatrix} M & & & \\ & M & & \\ & & \ddots & \ddots \\ & & & M \end{bmatrix}}_{\mathcal{M}} \begin{bmatrix} u_1 \\ u_2 \\ \vdots \\ u_{N_t} \end{bmatrix} + \Delta t \underbrace{\begin{bmatrix} B^T & 0 & \cdots \\ & B^T & \\ & & \ddots \\ & & & B^T \end{bmatrix}}_{\mathcal{C}^T} \begin{bmatrix} p_1 \\ p_2 \\ \vdots \\ p_{N_t} \end{bmatrix} = \begin{bmatrix} 0 \\ 0 \\ \vdots \\ 0 \end{bmatrix}.$$

In a vector notation we have

$$(48) \quad \alpha \Delta t \mathcal{M} \mathbf{u} + \Delta t \mathcal{C}^T \mathbf{p} = \mathbf{0}.$$

- *Adjoint equation:* we have to solve the first equation of the optimality system (6) at each time step as follows, considering  $M_s^T$  the matrix formulation of  $m_s^*$ :

$$M_s^T p_i = M_s^T p_{i+1} + \Delta t (-M_s^T y_i - K_s^T p_i + M_s^T y_{d_i}) \quad \text{for } i \in \{N_t - 1, N_t - 2, \dots, 1\}.$$

As did in previous steps, we derive the following block system:

$$\underbrace{\begin{bmatrix} M_s^T + \Delta t K_s^T & -M_s^T & & & \\ & \ddots & & & \\ & & M_s^T + \Delta t K_s^T & -M_s^T & \\ & & & \ddots & \\ & & & & M_s^T + \Delta t K_s^T \end{bmatrix}}_{\mathcal{A}_s^T} \mathbf{p} + \begin{bmatrix} \Delta t M_s^T y_1 \\ \vdots \\ \Delta t M_s^T y_{N_t} \end{bmatrix} = \begin{bmatrix} \Delta t M_s^T y_{d_1} \\ \vdots \\ \Delta t M_s^T y_{d_{N_t}} \end{bmatrix}.$$

Then, defining  $\mathcal{M}_s^T$  as the diagonal matrix in  $\mathbb{R}^{N \cdot N_t} \times \mathbb{R}^{N \cdot N_t}$  which diagonal entries are  $[M_s^T, \dots, M_s^T]$ , the adjoint system to be solved is:

$$\Delta t \mathcal{M}_s^T \mathbf{y} + \mathcal{A}_s^T \mathbf{p} = \Delta t \mathcal{M}_s^T \mathbf{y}_d.$$

In the end, we solve system (49) via an one shot approach:

$$(49) \quad \begin{bmatrix} \Delta t \mathcal{M}_s^T & 0 & \mathcal{A}_s^T \\ 0 & \alpha \Delta t \mathcal{M} & \Delta t \mathcal{C}^T \\ \mathcal{A}_s & \Delta t \mathcal{C}_s & 0 \end{bmatrix} \begin{bmatrix} \mathbf{y} \\ \mathbf{u} \\ \mathbf{p} \end{bmatrix} = \begin{bmatrix} \Delta t \mathcal{M}_s^T \mathbf{y}_d \\ 0 \\ \mathcal{M}_s \mathbf{y}_0 + \Delta t \mathbf{f}_s \end{bmatrix}.$$

#### 4. ROMS FOR ADVECTION-DOMINATED OCP( $\boldsymbol{\mu}$ )S

FEM simulations can be expensive in terms of computational time and memory storage: this issue is obviously more evident in case of high-dimensional discrete spaces. Moreover, when we talk about parametrized PDEs, one can require to repeat the simulations for several values of the parameter  $\boldsymbol{\mu}$ . To overcome these difficulties, we will use ROMs approach. The basic idea of ROMs is to create a low-dimensional space, called the *reduced space*, exploiting the parameter dependence of the problem at hand, such that it is a good approximation of the discrete initial space [8, 22, 41, 40, 39]. Let us consider a generic Parametrized OCPs described by the optimality conditions (6). We can define the set of the parametric solutions of the optimality system with respect to the functional space  $\mathbb{W} = Y \times U \times Q^*$  for steady OCP( $\boldsymbol{\mu}$ )s and  $\mathbb{W} = \mathcal{Y}_t \times \mathcal{U} \times \mathcal{Y}_t$  for the unsteady ones as

$$(50) \quad \mathbb{M} := \{(y(\boldsymbol{\mu}), u(\boldsymbol{\mu}), p(\boldsymbol{\mu})) \text{ solution of (6)} \mid \boldsymbol{\mu} \in \mathcal{P}\}.$$

The extension to space-time formulation for time-dependent problem is straightforward [6, 50] and requires small modifications, thus, we will exclusively refer to the steady framework.

**Assumption 4.0.1** (Smoothness of the solution manifold). *The continuous solution manifold  $\mathbb{M}$  is smooth with respect to the parameter  $\boldsymbol{\mu} \in \mathcal{P}$ .*

Let  $\mathbb{W}^N \subset \mathbb{W}$  be our FEM approximation of the continuous space  $\mathbb{W}$ , we call  $\mathbb{W}^N := Y^N \times U^N \times (Q^N)^*$  the high-fidelity space. Then, for stabilized problems we define the discrete parametric solution manifold as

$$(51) \quad \mathbb{M}^N := \{(y^N(\boldsymbol{\mu}), u^N(\boldsymbol{\mu}), p^N(\boldsymbol{\mu})) \text{ FEM solution of the (35)} \mid \boldsymbol{\mu} \in \mathcal{P}\}.$$

Starting from  $\mathbb{M}^N$ , ROM techniques create a reduced space of low dimension  $N$  denoted with  $\mathbb{W}^N$ , via a linear combination of *snapshots*, i.e. high-fidelity evaluations of the optimal solution  $(y^N(\boldsymbol{\mu}), u^N(\boldsymbol{\mu}), p^N(\boldsymbol{\mu}))$  computed in properly chosen parameters values  $\boldsymbol{\mu}$ . Obviously we have that  $\mathbb{W}^N \subset \mathbb{W}^N$  and we denote  $\mathbb{W}^N = Y^N \times U^N \times (Q^N)^*$ . Here,  $Y^N$ ,  $U^N$  and  $(Q^N)^*$  are the *reduced spaces* for the state, the control and the adjoint variables, respectively. The snapshots are collected by a POD algorithm using a *partitioned approach*. This strategy is followed due to good results shown in literature [28, 35, 49]. After having built these reduced function spaces, a standard Galerkin projection is performed onto these ones [5, 38, 42].

4.1. **Offline-Online Procedure for ROMs.** ROM procedure is divided in two stages:

- *offline* phase: here the *snapshots* are collected by solving the high-fidelity system (35). Secondly, the low-dimensional bases are created and hence all reduced spaces  $Y^N$ ,  $U^N$  and  $(Q^N)^*$  are built and stored, too. Moreover, all the  $\boldsymbol{\mu}$ -independent quantities are assembled and stored. It is potentially an expensive phase, which depends on  $\mathcal{N}$ .
- *online* phase: here a parameter  $\boldsymbol{\mu}$  is chosen and all the previous store  $\boldsymbol{\mu}$ -independent quantities are combined with the just-computed  $\boldsymbol{\mu}$ -dependent ones to build the reduced block matrix system based on a Galerkin projection. To be convenient, this phase should be  $\mathcal{N}$ -independent. Whereas in the offline phase stabilization is present due to stabilized snapshots, for the online phase this cannot be necessary. Therefore, we have two possibilities: if stabilization is performed also here, we talk about *Online-Offline stabilization*, otherwise we denote the setting as *Only-Offline stabilization*.

As already said, the online phase should be performed in a number of operations independent of  $\mathcal{N}$ . A sufficient condition is to admit the separation of the variables depending on  $\boldsymbol{\mu}$  and the solution  $(y, u, p)$  in the *affine decomposition* [22].

**Assumption 4.1.1.** *We require that all the forms in (35) are affine in  $\boldsymbol{\mu} \in \mathcal{P}$ .*

In Section 4.2 we describe the POD algorithm used in the offline phase. Now, we illustrate the explicit expression of the reduced solutions. Let us make clear the structure of the three reduced spaces in terms of their bases. Therefore, we define

$$(52) \quad \begin{aligned} Y^N &= \text{span} \{\eta_n^y, n = 1, \dots, N\}, & U^N &= \text{span} \{\eta_n^u, n = 1, \dots, N\}, \\ (Q^N)^* &= \text{span} \{\eta_n^p, n = 1, \dots, N\}, \end{aligned}$$

the reduced state, the reduced control and the reduced adjoint space, respectively. After having built them, we consider an enriched space for state and adjoint variables. Therefore, let us denote with  $\{\tau_n\}_{n=1}^{2N} = \{\eta_n^y\}_{n=1}^N \cup \{\eta_n^p\}_{n=1}^N$  the basis functions for the space  $Z^N$ , with  $Z^N \equiv Y^N \equiv (Q^N)^*$ , then we have  $Z^N = \text{span} \{\tau_n, n = 1, \dots, 2N\}$  [15, 19, 28, 29, 36, 35].

4.2. **Proper Orthogonal Decomposition.** In this Section we briefly describe the Proper Orthogonal Decomposition (POD) Galerkin algorithm [6, 22, 49, 50] for the construction of a discrete solution manifold and the relative reduced spaces. Since in the unsteady case we use a space-time structure, this procedure can be described making no distinction between time-dependency and steadiness. Firstly, we make a sampling of  $\mathcal{P}$  by choosing  $N_{\text{train}}$  of its elements. Therefore, let us define the set of the train samples as  $\mathcal{P}_{N_{\text{train}}}$ : we have that obviously  $\mathcal{P}_{N_{\text{train}}} \subset \mathcal{P}$  and the cardinality is  $|\mathcal{P}_{N_{\text{train}}}| = N_{\text{train}}$ . The set  $\mathcal{P}_{N_{\text{train}}}$  is denoted as the *training set*. We should pursue that  $N_{\text{train}}$  is large enough so as to ensure that  $\mathcal{P}_{N_{\text{train}}}$  is a good “approximation” of the parameter space  $\mathcal{P}$ .  $\mathcal{P}_{N_{\text{train}}}$  is built through a Monte-Carlo sampling method with respect to a uniform density with support equal to  $\mathcal{P}$ .

Starting from the sampling, the POD algorithm manipulates  $N_{\text{train}}$  snapshots for the state, the adjoint and the control variables:

$$(53) \quad \{(y^{\mathcal{N}}(\boldsymbol{\mu}_j), u^{\mathcal{N}}(\boldsymbol{\mu}_j), p^{\mathcal{N}}(\boldsymbol{\mu}_j))\}_{j=1}^{N_{\text{train}}} \text{ with } \boldsymbol{\mu}_j \in \mathcal{P}_{N_{\text{train}}}.$$

After this step, a compressing stage is performed: from (53) we build  $N$  basis functions by only considering the most important parametric information and throwing away the redundant ones, with  $N \leq N_{\text{train}}$ . A *partitioned approach* is used, which means that, after the deterministic sampling,

we perform the POD algorithm separately for all the three variables. Namely, we find three  $N$ -dimensional reduced spaces  $Y^N$ ,  $U^N$  and  $(Q^N)^*$  that minimizes the following three quantities:

$$\begin{aligned} & \sqrt{\frac{1}{N_{\text{train}}} \sum_{\boldsymbol{\mu}_j \in \mathcal{P}_{N_{\text{train}}}} \min_{\bar{y} \in Y^N} \|y^{\mathcal{N}}(\boldsymbol{\mu}_j) - \bar{y}\|_Y^2}, \\ & \sqrt{\frac{1}{N_{\text{train}}} \sum_{\boldsymbol{\mu}_j \in \mathcal{P}_{N_{\text{train}}}} \min_{\bar{u} \in U^N} \|u^{\mathcal{N}}(\boldsymbol{\mu}_j) - \bar{u}\|_U^2}, \\ & \sqrt{\frac{1}{N_{\text{train}}} \sum_{\boldsymbol{\mu}_j \in \mathcal{P}_{N_{\text{train}}}} \min_{\bar{p} \in (Q^N)^*} \|p^{\mathcal{N}}(\boldsymbol{\mu}_j) - \bar{p}\|_{Q^*}^2}, \end{aligned}$$

where obviously  $Y^N \subset Y^{\mathcal{N}}$ ,  $U^N \subset U^{\mathcal{N}}$  and  $(Q^N)^* \subset (Q^{\mathcal{N}})^*$ .

Let us discuss the data compression procedure of the POD for the state variable  $y(\boldsymbol{\mu})$  [6, 22, 49, 50]. As we are following a partitioned approach, the control and the adjoint variables follow the below discussion with usual modifications, as well. Firstly we collect a set of ordered parameters  $\boldsymbol{\mu}_1, \dots, \boldsymbol{\mu}_{N_{\text{train}}} \in \mathcal{P}_{N_{\text{train}}}$ , which the ordered snapshots  $y^{\mathcal{N}}(\boldsymbol{\mu}_1), \dots, y^{\mathcal{N}}(\boldsymbol{\mu}_{N_{\text{train}}})$  are linked to. Let us define  $\mathbf{C}^y \in \mathbb{R}^{N_{\text{train}} \times N_{\text{train}}}$  as the correlation matrix of the snapshots for the state variable as follows:

$$(54) \quad \mathbf{C}_{ij}^y := \frac{1}{N_{\text{train}}} (y^{\mathcal{N}}(\boldsymbol{\mu}_i), y^{\mathcal{N}}(\boldsymbol{\mu}_j))_Y, \quad 1 \leq i, j \leq N_{\text{train}}.$$

The next step is to find the pair eigenvalue-eigenvector  $(\lambda_n^y, e_n^y)$ , where  $e_n^y$  has norm equal to one, of the following problem:

$$\mathbf{C}^y e_n^y = \lambda_n^y e_n^y, \quad 1 \leq n \leq N_{\text{train}}.$$

For the sake of simplicity, we organise the eigenvalues  $\lambda_1^y, \dots, \lambda_{N_{\text{train}}}^y$  in decreasing order. Consider the first  $N$  ones, specifically  $\lambda_1^y, \dots, \lambda_N^y$  together with the related eigenvectors  $e_1^y, \dots, e_N^y$ . We refer to the  $k$ -th component of the state eigenvector  $e_n^y \in \mathbb{R}^{N_{\text{train}}}$  with the notation  $(e_n^y)_k$ . After having finished the computation of the pair eigenvalue-eigenvector, the basis functions  $\eta_n^y$  for the state equation are built through the following formula:

$$(55) \quad \eta_n^y = \frac{1}{\sqrt{\lambda_n^y}} \sum_{k=1}^{N_{\text{train}}} (e_n^y)_k y^{\mathcal{N}}(\boldsymbol{\mu}_k), \quad 1 \leq n \leq N.$$

Therefore, our reduced spaces are built as (52) and, then, aggregated space technique is applied.

As both  $N$  and  $N_{\text{train}}$  can be chosen by us, we should find sharp criteria in order to decide them. A possibility can be to set them in based on a study of the eigenvalues, using the estimate [22, 39, 58]:

$$(56) \quad \sqrt{\frac{1}{N_{\text{train}}} \sum_{k=1}^{N_{\text{train}}} \|y^{\mathcal{N}}(\boldsymbol{\mu}_k) - \Pi^N(y^{\mathcal{N}}(\boldsymbol{\mu}_k))\|_Y^2} = \sqrt{\sum_{k=N+1}^{N_{\text{train}}} \lambda_k^y},$$

where  $\Pi^N : Y \rightarrow Y^N$  is a Galerkin projector of functions from  $Y$  onto  $Y^N$ . (56) holds for the control and the adjoint in a partitioned approach, too. The second member of equation (56) can be a measure of how well the FEM space is approximated by  $N$  reduced basis over the chosen training set of cardinality  $N_{\text{train}}$ . We summarise the whole POD procedure in the below Algorithm 1.

**Remark 4.2.1** (Time-dependent problems). *When we are dealing with time-dependent OCPs, the time instances are not separated in the POD procedure. Therefore, the space-time problem is studied as a steady one and each snapshot carries all the time instances.*

---

**Algorithm 1** POD algorithm for OCP problems in a partitioned approach

---

**Input:** parameter domain  $\mathcal{P}$ , FEM spaces  $Y^{\mathcal{N}}$ ,  $U^{\mathcal{N}}$  and  $(Q^{\mathcal{N}})^*$  and  $N_{\text{train}}$ .

**Output:** reduced spaces  $Y^N$ ,  $U^N$  and  $(Q^N)^*$ .

Starting from the high-fidelity spaces  $Y^{\mathcal{N}}$ ,  $U^{\mathcal{N}}$  and  $(Q^{\mathcal{N}})^*$ :

- 1: Sample  $\mathcal{P}_{\text{train}} \subset \mathcal{P}$ ;
  - 2: **for all**  $\boldsymbol{\mu} \in \mathcal{P}_{\text{train}}$  **do**
  - 3:     Solve the high-fidelity OCP system (34) (in this case a stabilized one);
  - 4: **end for**
  - 5: Assemble the matrix  $\mathbf{C}_{ij}^y := \frac{1}{N_{\text{train}}} (y^{\mathcal{N}}(\boldsymbol{\mu}_i), y^{\mathcal{N}}(\boldsymbol{\mu}_j))_Y$ ,  $1 \leq i, j \leq N_{\text{train}}$ . Do the same for  $u$  and  $p$  variables;
  - 6: Compute its eigenvalues  $\lambda_1^y, \dots, \lambda_{N_{\text{train}}}^y$  and the corresponding orthonormalised eigenvectors  $e_1^y, \dots, e_{N_{\text{train}}}^y$ . Do the same for  $u$  and  $p$  variables;
  - 7: After having chosen  $N$  according to a certain criterion, define  $Y^N = \text{span} \{\eta_n^y, n = 1, \dots, N\}$ , where  $\eta_n^y = \frac{1}{\sqrt{\lambda_n^y}} \sum_{k=1}^{N_{\text{train}}} (e_n^y)_k y^{\mathcal{N}}(\boldsymbol{\mu}_k)$ . Do the same for  $u$  and  $p$  variables.
  - 8: Define the aggregated space  $Z^N = \text{span} \{ \{\eta_n^y\}_{n=1}^N \cup \{\eta_n^p\}_{n=1}^N \}$  and impose  $Z^N \equiv Y^N \equiv (Q^N)^*$ .
- 

## 5. NUMERICAL RESULTS

In this Section we propose simulations regarding the Graetz-Poiseuille and the Propagating Front in a Square problems. Regarding the steady case, the numerical experiments are coded through the RBniCS library [2]; instead, the unsteady ones are implemented employing both RBniCS and multiphenics [1] libraries. They are python-based libraries, built on FEniCS [32].

When we will perform the Online-Offline stabilization procedure, we will always use the same stabilization parameter  $\delta_K$  of the high-fidelity approximation also at the reduced level, both in steady and unsteady cases.

We will illustrate an analysis over *relative errors* between the FEM and the reduced solutions for all three variables, defined as

$$(57) \quad e_{y,N}(\boldsymbol{\mu}) := \frac{\|y^{\mathcal{N}}(\boldsymbol{\mu}) - y^N(\boldsymbol{\mu})\|_Y}{\|y^{\mathcal{N}}(\boldsymbol{\mu})\|_Y}, \quad e_{u,N}(\boldsymbol{\mu}) := \frac{\|u^{\mathcal{N}}(\boldsymbol{\mu}) - u^N(\boldsymbol{\mu})\|_U}{\|u^{\mathcal{N}}(\boldsymbol{\mu})\|_U}, \quad e_{p,N}(\boldsymbol{\mu}) := \frac{\|p^{\mathcal{N}}(\boldsymbol{\mu}) - p^N(\boldsymbol{\mu})\|_{Q^*}}{\|p^{\mathcal{N}}(\boldsymbol{\mu})\|_{Q^*}},$$

for the state, the control and the adjoint, respectively. As we are dealing with parametrized OCPs, we will evaluate a simple average of (57) for  $\boldsymbol{\mu}$  uniformly distributed in a testing set  $\mathcal{P}_{\text{test}} \subseteq \mathcal{P}$  of size  $N_{\text{test}}$  for every dimension  $N = 1, \dots, N_{\text{max}}$  of the reduced space obtained by our POD procedure. More precisely, we will plot the base-10 logarithm of the average of (57). For parabolic problems we will consider the sum of the errors with respect to each discretized instant of time  $t$ .

Regarding the efficiency of ROMs, we use the *speedup-index* to compare the computational cost of the FEM solution with that of the reduced one. This quantity is defined as:

$$(58) \quad \text{speedup-index} = \frac{\text{computational time of the high-fidelity solution}}{\text{computational time of the reduced solution}},$$

which will be computed for each  $\boldsymbol{\mu}$  in the testing set with respect to the dimension  $N$  of the reduced spaces. As made with the relative error, we will consider the sample average of this quantity with respect to  $N$ ; however, for the sake of completeness, we will add its minimum and maximum value computed through the testing set. For each test case, we will use the same  $\mathcal{P}_{\text{test}}$  to compute relative errors and the speedup-index. The steady results are obtained with 16GB of RAM and Intel Core i7-7500U Dual Core, 2.7GHz for the CPU; instead, the FEM and ROM parabolic simulations are run with 16GB of RAM and Intel Core i7 – 7700 Quad Core, 3.60GHz for the CPU.

**5.1. Numerical Experiments for the Graetz-Poiseuille Problem.** The Graetz-Poiseuille problem concerns the heat conduction in a straight duct, whose walls can be characterized by heat



exchange or maintained at a certain fixed temperature. This example is very well-known in the numerical Advection-Dominated literature [18, 37, 44, 55]. We start by presenting the stationary case. We apply a distributed control in the whole domain and the parameter  $\boldsymbol{\mu} = \mu_1 > 0$  is a physical component and characterizes the diffusion term. The spatial coordinates of the system are denoted

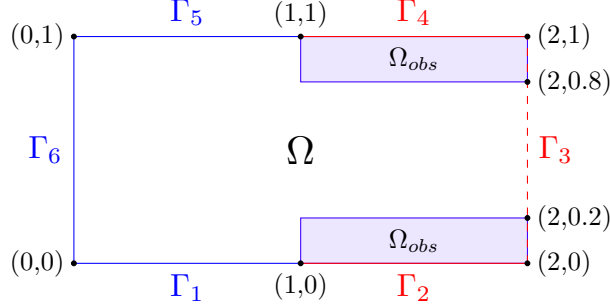


**Figure 1.** Geometry of the Graetz-Poiseuille Problem.

with  $(x_0, x_1)$ . The boundary of  $\Omega$  is  $\Gamma$ . We consider Dirichlet boundary conditions (BC) on sides  $\Gamma_1 := [0, 1] \times \{0\}$ ,  $\Gamma_5 := [0, 1] \times \{1\}$ ,  $\Gamma_6 := \{0\} \times [0, 1]$  by imposing  $y = 0$  and  $\Gamma_2 := [1, 2] \times \{0\}$  and  $\Gamma_4 := [1, 2] \times \{1\}$  by imposing  $y = 1$ , referring to Figure 1. We deal with homogeneous Neumann conditions on  $\Gamma_3 := \{2\} \times [0, 1]$ . The classic formulation of the problem is:

$$(59) \quad \begin{cases} -\frac{1}{\mu_1} \Delta y(\boldsymbol{\mu}) + 4x_1(1-x_1)\partial_{x_0}y(\boldsymbol{\mu}) = u, & \text{in } \Omega, \\ y(\boldsymbol{\mu}) = 0, & \text{on } \Gamma_1 \cup \Gamma_5 \cup \Gamma_6, \\ y(\boldsymbol{\mu}) = 1, & \text{on } \Gamma_2 \cup \Gamma_4, \\ \frac{\partial y(\boldsymbol{\mu})}{\partial \nu} = 0, & \text{on } \Gamma_3. \end{cases}$$

Now we want to derive the optimality system.  $\Omega_{obs} := [1, 2] \times [0.8, 1] \cup [1, 2] \times [0, 0.2]$  as illustrated in Figure 1. In this case, the state belongs to the space:

$$\tilde{Y} := \{v \in H^1(\Omega) \text{ s.t. it satisfies the BC in (59)}\}.$$

For the sake of practice, it is better to introduce a lifting function  $R_y \in H^1(\Omega)$ , such that it fulfills the BC in (59). Therefore we define the variable  $\bar{y} := y - R_y$ , with  $\bar{y} \in Y$ , where

$$Y := \{v \in H_0^1(\Omega) \text{ s.t. } \frac{\partial \bar{y}}{\partial \nu} = 0, \text{ on } \Gamma_3 \text{ and } \bar{y} = 0 \text{ on } \Gamma \setminus \Gamma_3\}.$$

Nevertheless, without loss of generality, we will denote the new variable  $\bar{y}$  with  $y$  and we settle  $U := L^2(\Omega)$  and  $Q := Y^*$ . Therefore, the adjoint variable  $p$  is null on  $\Gamma \setminus \Gamma_3$ . The mathematical formulation is described as follows (we omitted the dependence from  $\boldsymbol{\mu}$ ). Fixed  $\alpha > 0$ , find the pair  $(y, u) \in Y \times U$  that realizes

$$(60) \quad \min_{(y,u) \in Y \times U} J(y, u) = \frac{1}{2} \int_{\Omega_{obs}} (y - y_d)^2 \, dx + \frac{\alpha}{2} \int_{\Omega} u^2 \, dx \quad \text{such that } e(y, u, p; \boldsymbol{\mu}) = 0,$$

where  $e(y, u, p; \boldsymbol{\mu}) := a(y, p; \boldsymbol{\mu}) + b(u, p; \boldsymbol{\mu}) - \langle p, f(\boldsymbol{\mu}) \rangle_{Y^*Y}$ . As explained in Sections 2 and 3, we follow a Lagrangian approach and we use SUPG stabilization in a *optimize-then-discretize* framework. We exploit  $\mathbb{P}^1$ -FEM approximation for the state, control and adjoint spaces. Here the stabilized forms  $a_s$  and  $a_s^*$  are, respectively:

$$a_s(y^{\mathcal{N}}, q^{\mathcal{N}}; \boldsymbol{\mu}) := a(y^{\mathcal{N}}, q^{\mathcal{N}}; \boldsymbol{\mu}) + \sum_{K \in \mathcal{T}_h} \delta_K \int_K (4x_1(1-x_1)\partial_{x_0}y^{\mathcal{N}}) (h_K \partial_{x_0}q^{\mathcal{N}}), \quad y^{\mathcal{N}}, q^{\mathcal{N}} \in Y^{\mathcal{N}},$$

$$a_s^*(z^{\mathcal{N}}, p^{\mathcal{N}}; \boldsymbol{\mu}) := a^*(z^{\mathcal{N}}, p^{\mathcal{N}}; \boldsymbol{\mu}) + \sum_{K \in \mathcal{T}_h} \delta_K \int_K (4x_1(1-x_1)\partial_{x_0}p^{\mathcal{N}}) (h_K \partial_{x_0}z^{\mathcal{N}}), \quad z^{\mathcal{N}}, p^{\mathcal{N}} \in Y^{\mathcal{N}}.$$

We consider a parameter space  $\mathcal{P} := [10^4, 10^6]$  and a quite coarse mesh of size  $h = 0.029$  for the FEM spaces. The training set  $\mathcal{P}_{\text{train}}$  has cardinality  $N_{\text{train}} = 100$ . We choose  $\delta_K = 1.0$  for all  $K \in \mathcal{T}_h$  and the penalization term is  $\alpha = 0.01$ . We pursue the convergence in the  $L^2$ -norm of the state to the desired solution profile  $y_d(x) = 1.0$ , function defined on  $\Omega_{\text{obs}}$  of Figure 1. We perform the POD algorithm for  $N_{\text{max}} = 20$  in a partitioned approach. We illustrate the reduced solution for the state and adjoint variables in the best relative error scenario in Figure 2. Namely, we plot the Only-Offline and Online-Offline Stabilized solutions for  $N = 1$  and  $N = 6$ . The values of  $N$  can be deduced by Figure 3. From the gradient equation (34), we expect the distributed control  $u$  to be equal to the adjoint  $p$  up to the multiplicative constant  $\alpha$ .

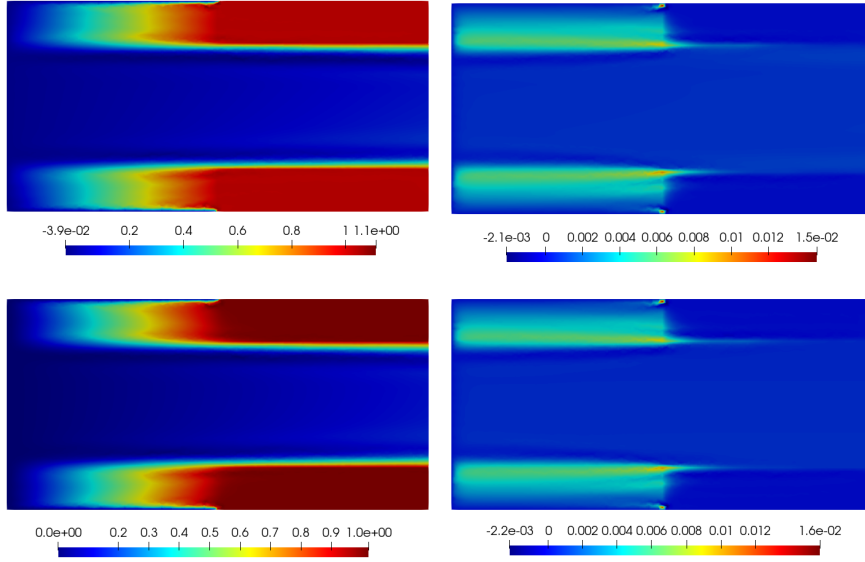


**Figure 2.** (Top) Only-Offline stabilized state (left) and adjoint (right) for  $N = 1$ ; (Bottom) Online-Offline stabilized state (left) and adjoint (right) for  $N = 6$ ; for the Graetz-Poiseuille Problem;  $\mathcal{P} = [10^4, 10^6]$ ,  $\mu_1 = 10^5$ ,  $h = 0.029$ ,  $\delta_K = 1.0$ ,  $\alpha = 0.01$ .

We consider the relative errors between the FEM and the reduced solution in Figure 3. We use a testing set  $\mathcal{P}_{\text{test}}$  of 100 elements in  $\mathcal{P}$ . As previously cited, at  $N = 6$  we reach the minima for all the three errors for the Online-Offline stabilization; more precisely for the state we touch  $e_{y,6} = 9.65 \cdot 10^{-9}$ , for the adjoint  $e_{p,6} = 1.98 \cdot 10^{-8}$  and the control  $e_{u,6} = 6.00 \cdot 10^{-9}$ . In contrast with this situation, Only-Offline stabilization never falls under  $10^{-2}$ . This implies that the best choice is to pursue the Online-Offline stabilization procedure for this problem. However, after  $N = 6$  the errors begin slightly to increase. Our interpretation to this fact relies on  $\mathcal{P}$ . Despite the fact that this parameter space might be too large, however the coefficient which multiplies the diffusion operator is still absolutely low in value for every  $\mu_1 \in \mathcal{P}$ , nearly  $10^{-4}$  and  $10^{-5}$ . Therefore, also thanks to SUPG stabilization and the distributed control action, the majority of snapshots can be very similar referring to the solution for  $\mu_1 = 10^5$ : this translates in very few bases to reach a good relative error. As a matter of fact, the eigenvalues  $\lambda_7^y, \lambda_7^u$  are  $\approx 10^{-15}$  and  $\lambda_7^p \approx 10^{-16}$ ; by their decreasing order, all the subsequent eigenvalues are very close to zero machine. Thus, recalling (55) it follows that all basis components with  $N \geq 7$  are affected by some rounding errors due to the orthonormalization procedure of the POD (for details see [39]).

Finally, we take a look at the speedup-index in Table 1. All the average values are better for the Only-Offline stabilized ROM procedure due to the fact that the stabilized forms are not taken into account in the online phase. However, the Online-Offline stabilized reduced solution shows very good behaviour, for instance, we have an average equal to 284.3 for  $N = 6$ . Generally, in this case speedup-index takes average value around  $2 \cdot 10^2$  order of magnitude for the first 20 basis elements.

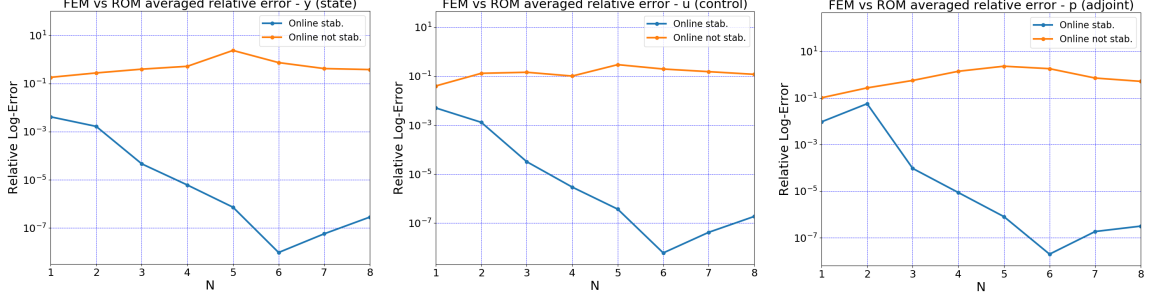


**Figure 3.** Relative errors between FEM and reduced solution for state (left), control (center) and adjoint (right), for Online-Offline and Only-Offline stabilization,  $\alpha = 0.01$ ,  $N_{\text{test}} = 100$ ,  $h = 0.029$ ,  $\mathcal{P} = [10^4, 10^6]$ . Graetz-Poiseuille Problem.

$N$	Only-Offline Stabilization			Offline-Online Stabilization		
	min	average	max	min	average	max
1	162.1	296.6	338.1	170.8	261.7	285.9
2	172.2	342.1	391.3	178.4	298.5	327.1
3	168.5	336.2	383.7	192.0	298.9	325.3
4	165.1	336.1	385.6	256.7	298.0	322.6
5	164.8	331.6	376.6	220.1	287.6	307.7
6	198.3	321.0	366.4	192.3	284.3	305.7
7	186.1	318.4	348.6	228.6	282.6	306.9

**Table 1.** Speedup-index of the Graetz-Poiseuille Problem for Online-Offline and Only-Offline stabilizations with  $\mathcal{P}_{\text{test}}$  sampled from  $\mathcal{P} = [10^4, 10^6]$ ,  $N_{\text{test}} = 100$ ,  $\alpha = 0.01$ ,  $h = 0.029$ ,  $\delta_K = 1.0$ ,  $\alpha = 0.01$ .

Let us give a look to the unsteady version of Problem (59) with null initial condition. The unsteady Graetz-Poiseuille problem without control has been presented in [37, 55], instead the OCP Graetz Problem under boundary control without Advection-dominancy is studied in [50, 48].

Recalling Figure 1, for a fixed  $T > 0$  we state the parabolic Graetz-Poiseuille Problem as follows:

$$(61) \quad \begin{cases} \frac{\partial y(\boldsymbol{\mu})}{\partial t} - \frac{1}{\mu_1} \Delta y(\boldsymbol{\mu}) + 4x_1(1-x_1)\partial_{x_0} y(\boldsymbol{\mu}) = u, & \text{in } \Omega \times (0, T), \\ y(\boldsymbol{\mu}) = 0, & \text{on } \Gamma_1 \cup \Gamma_5 \cup \Gamma_6 \times (0, T), \\ y(\boldsymbol{\mu}) = 1, & \text{on } \Gamma_2 \cup \Gamma_4 \times (0, T), \\ \frac{\partial y(\boldsymbol{\mu})}{\partial \nu} = 0, & \text{on } \Gamma_3 \times (0, T), \\ y(\boldsymbol{\mu})(0) = 0, & \text{in } \Omega. \end{cases}$$

We do simulations in a space-time framework as discussed in Section 3.2 for a prearranged number of time-steps  $N_t$  using a  $\mathbb{P}^1$ -FEM approximation for the high-fidelity solutions. The relative stabilized forms in (49) for derivatives along time for state and adjoint are, respectively:

$$(62) \quad \begin{aligned} m_s(y^N, q^N; \boldsymbol{\mu}) &= (y^N, q^N)_{L^2(\Omega)} + \sum_{K \in \mathcal{T}_h} \delta_K h_K (y^N, \partial_{x_0} q^N)_K, \quad y^N, q^N \in Y^N, \\ m_s^*(p^N, z^N; \boldsymbol{\mu}) &= (p^N, z^N)_{L^2(\Omega)} - \sum_{K \in \mathcal{T}_h} \delta_K h_K (p^N, \partial_{x_0} z^N)_K, \quad p^N, z^N \in Y^N. \end{aligned}$$

We consider a final time of  $T = 3.0$  and a time step of  $\Delta t = 0.1$ , hence we have  $N_t = 30$ . We choose a quite coarse mesh of  $h = 0.038$  and the overall high-fidelity dimension is  $\mathcal{N}_{\text{tot}} = 314820$ . This means that a single FEM space for a fixed  $t$  has a dimension of  $\mathcal{N} = 3498$ . We consider a initial condition of  $y_0(x) = 0$  for all  $x \in \Omega$  referring to Figure 1. We want the state solution to converge

in the  $L^2$ -norm to a desired solution profile  $y_d(x, t) = 1.0$ , function defined for all  $t \in [0, 3.0]$  and for all  $x$  in  $\Omega_{obs}$ . Here the SUPG stabilization is implemented with parameters  $\delta_K = 1.0$  for all  $K \in \mathcal{T}_h$ .  $\mathcal{P} := [10^4, 10^6]$  and we choose a training set  $\mathcal{P}_{train}$  of cardinality  $N_{train} = 100$ . Then, we performed the POD algorithm with  $N_{max} = 20$ . The penalization parameter is  $\alpha = 0.01$ .

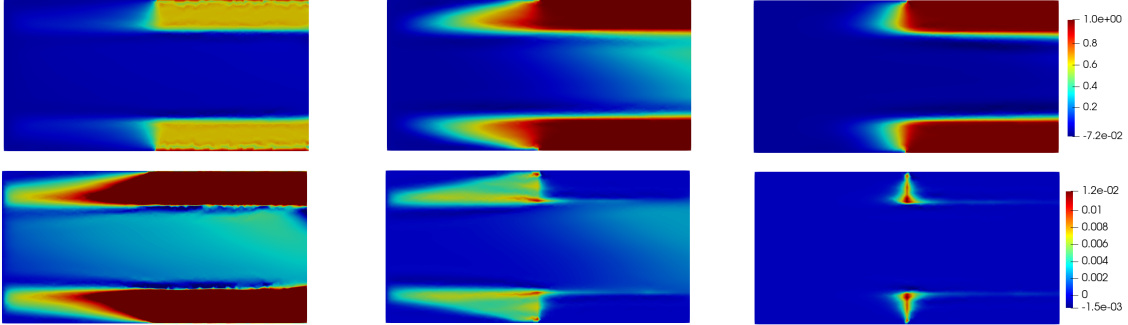


**Figure 4.** (Top) SUPG FEM solution for the state and (Bottom) for the adjoint at  $t = 0.1$ ,  $t = 1.5$ ,  $t = 3.0$ . Unsteady Graetz-Poiseuille Problem,  $\mu_1 = 10^5$ ,  $N_t = 30$ ,  $h = 0.038$ ,  $\delta_K = 1.0$ ,  $\alpha = 0.01$ .

As we will see in Figure 5 the performance of the Only-Offline stabilized reduced solutions are not so good in terms of accuracy, unlike the Online-Offline stabilized ones. We consider a testing set of 100 elements in  $\mathcal{P}$ . As succeeded in the steady case in Section 5.1, after nearly  $N = 6$  Online-Offline stabilized errors begin to fluctuate due to the nature of the eigenvalues of the correlation matrix (54) that are closed to zero machine. For this reason we present the trend of error from 1 to 10. However, errors stays close to  $10^{-7}$  for the state and the adjoint and  $10^{-6}$  to the control. For  $N = 6$  we have  $e_{y,6} = 4.20 \cdot 10^{-7}$ ,  $e_{u,6} = 1.10 \cdot 10^{-6}$  and  $e_{p,6} = 3.18 \cdot 10^{-7}$ , instead for  $N = 20$  we have  $e_{y,20} = 1.93 \cdot 10^{-7}$ ,  $e_{u,20} = 3.25 \cdot 10^{-7}$  and  $e_{p,20} = 1.21 \cdot 10^{-7}$  for the Online-Offline stabilization ROM.

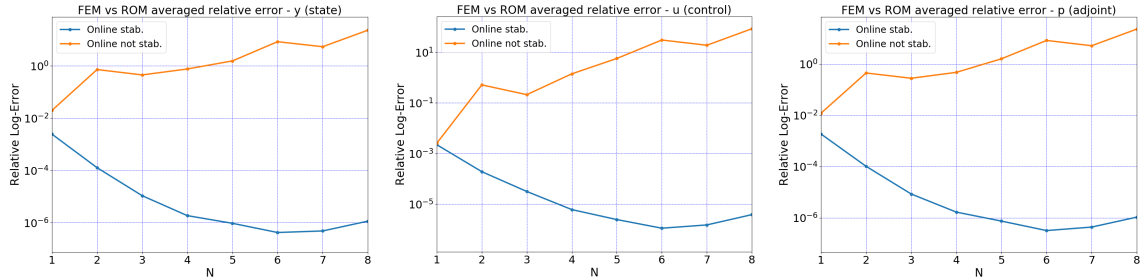


**Figure 5.** Relative errors between the FEM and Only-Offline and Online-Offline stabilized solutions for the state (left), control (center) and adjoint (right), Unsteady Graetz-Poiseuille problem,  $N_t = 30$ ,  $N_{test} = 100$ ,  $\mathcal{P} = [10^4, 10^6]$ ,  $h = 0.038$ .

Finally, we can see the speedup-index for some value of  $N$  in Table 2. In both situation we can compute a huge number of reduced solutions in the time of a high-fidelity one: for the Offline-Online stabilization we have an average speedup-index of nearly 26000 for  $N = 6$ . On the whole, average speedup-index has an order of magnitude of  $2 \cdot 10^4$  for  $N \leq 20$ .

**5.2. Numerical Experiments for Propagating Front in a Square Problem.** In this Section, we consider a problem studied in the Advection-Dominated form in [37, 55] from a numerical point of view and we will add a distributed control to it. Let  $\Omega$  be the unit square in  $\mathbb{R}^2$ . We consider the representation in Figure 6. Also in this case,  $(x_0, x_1)$  are the coordinates of the square domain.

$N$	Only-Offline Stabilization			Offline-Online Stabilization		
	min	average	max	min	average	max
1	21588.3	26588.8	30971.5	18968.4	23588.0	27062.7
2	23821.3	29723.4	34817.2	20757.2	26018.9	29929.1
3	23571.0	29468.6	34349.5	20547.9	25698.2	29662.5
4	23062.2	28880.6	33702.7	21385.2	25380.9	28883.3
5	25762.9	28767.9	33488.8	23021.5	25882.4	29388.9
6	27003.2	29707.7	34544.7	23236.5	26054.7	29677.5
7	26658.5	29481.1	34277.3	23206.6	25879.5	29505.4

**Table 2.** Speedup-index of the Unsteady Graetz Problem for Online-Offline and Only-Offline stabilization with  $\mathcal{P} = [10^4, 10^6]$ ,  $\alpha = 0.01$ ,  $N_t = 30$ ,  $N_{\text{test}} = 100$ ,  $h = 0.038$ .

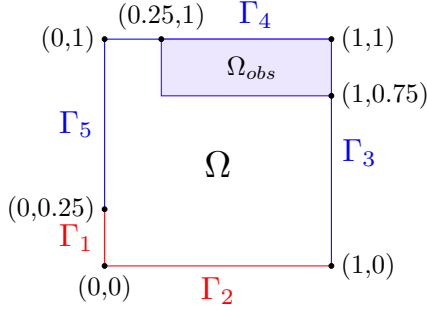


**Figure 6.** Geometry of the Square Problem

Referring to Figure 6,  $\Gamma_1 := \{0\} \times [0, 0.25]$ ,  $\Gamma_2 := [0, 1] \times \{0\}$ ,  $\Gamma_3 := \{1\} \times [0, 1]$ ,  $\Gamma_4 := [0, 1] \times \{1\}$ ,  $\Gamma_5 := \{0\} \times [0.25, 1]$ ;  $\Omega_{obs} := [0.25, 1] \times [0.75, 1]$ . Given  $\boldsymbol{\mu} = (\mu_1, \mu_2)$ , the problem is formulated as

$$(63) \quad \begin{cases} -\frac{1}{\mu_1} \Delta y(\boldsymbol{\mu}) + (\cos \mu_2, \sin \mu_2) \cdot \nabla y(\boldsymbol{\mu}) = u, & \text{in } \Omega, \\ y(\boldsymbol{\mu}) = 1, & \text{on } \Gamma_1 \cup \Gamma_2, \\ y(\boldsymbol{\mu}) = 0, & \text{on } \Gamma_3 \cup \Gamma_4 \cup \Gamma_5. \end{cases}$$

We assume that the Identity restricted to  $\Omega_{obs}$  as the Observation operator and  $Z := L^2(\Omega_{obs})$ . In our test cases,  $\mathcal{P} := [10^4, 10^5] \times [0, 1.57]$ . In this case, we have that the domain of definition of our state  $y$  is

$$\tilde{Y} := \{v \in H^1(\Omega) \text{ s.t. BC in (63)}\}.$$

Exactly as done in the previous paragraph, we define a lifting function  $R_y \in H^1(\Omega)$  such that satisfies BC in (63). We define  $\bar{y} := y - R_y$ , even though we denote  $\bar{y}$  as  $y$  again for the sake of notation. We consider  $Y := H_0^1(\Omega)$ ,  $U = L^2(\Omega)$  and  $Q := Y^*$ , hence the adjoint  $p$  is such that  $p = 0$  on  $\partial\Omega$ . We define the objective functional  $J$  exactly as in (60); instead,  $a$  and  $b$  are

$$a(y, p; \boldsymbol{\mu}) := \int_{\Omega} \frac{1}{\mu_1} \nabla y \cdot \nabla p + (\cos \mu_2, \sin \mu_2) \cdot \nabla y p \, dx, \quad \text{and } b(u, p; \boldsymbol{\mu}) := - \int_{\Omega} u p \, dx.$$

and  $\langle p, f(\boldsymbol{\mu}) \rangle_{Y^*Y} = -a(R_y, p; \boldsymbol{\mu})$ . Then we follow usual discussions of Sections 2 and 3.

We exploit a  $\mathbb{P}^1$ -FEM approximation for the optimality system by using the usual SUPG stabilization technique, arriving to system (34). Here, for the sake of completeness, we remark that the

stabilized forms  $a_s$  and  $a_s^*$  are, respectively:

$$a_s(y^{\mathcal{N}}, q^{\mathcal{N}}; \boldsymbol{\mu}) := a(y^{\mathcal{N}}, q^{\mathcal{N}}; \boldsymbol{\mu}) + \sum_{K \in \mathcal{T}_h} \delta_K \int_K h_K (\cos \mu_2, \sin \mu_2) \cdot \nabla y^{\mathcal{N}} (\cos \mu_2, \sin \mu_2) \cdot \nabla q^{\mathcal{N}},$$

$$a_s^*(z^{\mathcal{N}}, p^{\mathcal{N}}; \boldsymbol{\mu}) := a^*(z^{\mathcal{N}}, p^{\mathcal{N}}; \boldsymbol{\mu}) + \sum_{K \in \mathcal{T}_h} \delta_K \int_K h_K (\cos \mu_2, \sin \mu_2) \cdot \nabla p^{\mathcal{N}} (\cos \mu_2, \sin \mu_2) \cdot \nabla z^{\mathcal{N}},$$

for all  $y^{\mathcal{N}}, q^{\mathcal{N}}, z^{\mathcal{N}}, p^{\mathcal{N}} \in Y^{\mathcal{N}}$ . As previously done, we build a training set  $\mathcal{P}_{\text{train}}$  and a testing set  $\mathcal{P}_{\text{test}}$  with both cardinality  $n_{\text{train}} = 100$ . The mesh size  $h$  is 0.025 and therefore the overall dimension of the high-fidelity approximation is 12087, which implies that state, control and adjoint spaces have dimension equal  $\mathcal{N} = 4029$ . The SUPG stabilization is implemented with parameters  $\delta_K = 1.0$  for all  $K \in \mathcal{T}_h$ . The penalization parameter is  $\alpha = 0.01$  and we pursue the state solution to be convergent in the  $L^2$ -norm to a desired solution profile  $y_d(x) = 0.5$ , defined for all  $x$  in  $\Omega_{\text{obs}}$  of Figure 6. In Figure 7 we observe state and adjoint FEM solutions for  $\boldsymbol{\mu} = (2 \cdot 10^4, 1.2)$ . Instead, in Figure 8 we illustrate Only-Offline and Online-Offline reduced solution for the state and the adjoint variable with  $\boldsymbol{\mu} = (2 \cdot 10^4, 1.2)$  for  $N = 50$ .

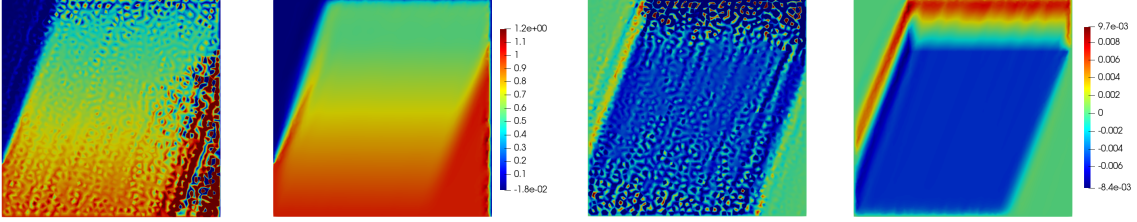


**Figure 7.** Numerical solution without stabilization and SUPG FEM solution with  $\boldsymbol{\mu} = (2 \cdot 10^4, 1.2)$  for state (left) and adjoint (right) variables in the Propagating Front in a Square Problem,  $\alpha = 0.01$ ,  $h = 0.025$ ,  $\delta_K = 1.0$ .

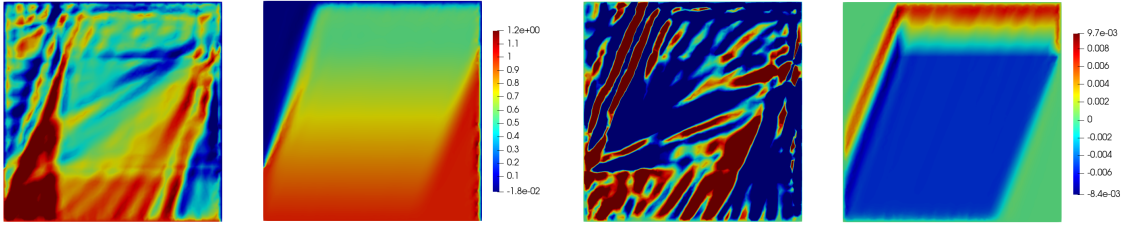


**Figure 8.** Only-Offline stabilized and Online-Offline stabilized reduced solutions with  $\boldsymbol{\mu} = (2 \cdot 10^4, 1.2)$  for state (left) and adjoint (right) variables in the Propagating Front in a Square Problem,  $\alpha = 0.01$ ,  $N = 50$ ,  $h = 0.025$ ,  $\delta_K = 1.0$ ,  $\mathcal{P} = [10^4, 10^5] \times [0, 1.57]$ .

These computational evidences and the analysis of the relative errors show that Online-Offline stabilization procedure is preferable in this setting. In Figure 9, the trend is the same of all three variables, where errors continue to decrease along all  $N$ : we have  $e_{y,50} = 1.20 \cdot 10^{-3}$ ,  $e_{u,50} = 7.67 \cdot 10^{-4}$  and  $e_{p,50} = 3.16 \cdot 10^{-3}$ .

Concerning the speedup-index, the performance are quite good as seen in Table 3. For the best approximation, we have that we can compute an average of 44 Online-Offline reduced solutions when we build the associated FEM one. Obviously, the Only-Offline stabilized one is slightly better. On the whole, speedup-index takes average value around  $10^1, 10^2$  order of magnitude for  $N \leq 50$ .

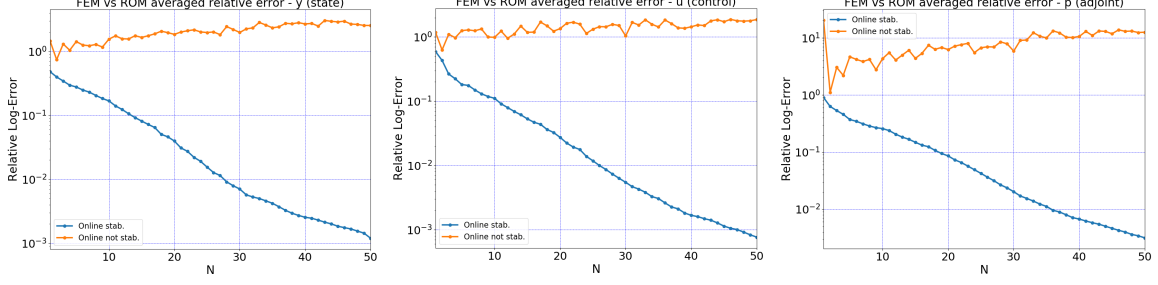


**Figure 9.** Relative errors between FEM and reduced solutions with  $\mathcal{P} = [10^4, 10^5] \times [0, 1.57]$  for the state (left), control (center) and adjoint (right) in the Propagating Front in a Square Problem,  $N_{\text{test}} = 100$ ,  $\alpha = 0.01$ ,  $h = 0.025$ ,  $\delta_K = 1.0$ .

$N$	Only-Offline Stabilization			Offline-Online Stabilization		
	min	average	max	min	average	max
1	123.1	198.8	243.1	110.0	162.7	181.9
10	132.2	200.4	244.2	110.8	158.3	176.9
20	84.6	158.3	191.7	60.1	124.3	141.3
30	78.8	114.7	137.8	65.0	92.5	104.7
40	54.2	78.6	96.1	46.9	64.2	72.3
50	33.2	53.0	64.8	28.5	44.0	49.9

**Table 3.** Speedup-index of the Propagating Front in a Square Problem for Online-Offline and Only-Offline stabilization with training set  $\mathcal{P} = [10^4, 10^5] \times [0, 1.57]$ ,  $\alpha = 0.01$ ,  $N_{\text{test}} = 100$ ,  $h = 0.025$ ,  $\delta_K = 1.0$ .

Now we study the unsteady case of the Propagating Front in a Square Problem for a fix  $T > 0$ :

$$(64) \quad \begin{cases} \frac{\partial y(\boldsymbol{\mu})}{\partial t} - \frac{1}{\mu_1} \Delta y(\boldsymbol{\mu}) + (\cos \mu_2, \sin \mu_2) \cdot \nabla y(\boldsymbol{\mu}) = u, & \text{in } \Omega \times (0, T), \\ y(\boldsymbol{\mu}) = 1, & \text{on } \Gamma_1 \cup \Gamma_2 \times (0, T), \\ y(\boldsymbol{\mu}) = 0, & \text{on } \Gamma_3 \cup \Gamma_4 \cup \Gamma_5 \times (0, T), \\ y(\boldsymbol{\mu})(0) = 0, & \text{in } \Omega, \end{cases}$$

with initial value  $y_0(x) = 0$  for all  $x \in \Omega$  referring to the domain in Figure 6. We build a parabolic problem for a final time  $T = 3.0$  and a time-step  $\Delta t = 0.1$ , hence  $N_t = 30$ . We choose a quite coarse mesh of size  $h = 0.036$  and the overall dimension of the space-time system is  $N_{\text{tot}} = 174780$ , which means that a single FEM space has dimension  $\mathcal{N} = 1942$ . Again, our aim is to achieve in a  $L^2$ -mean a desired solution profile  $y_d(x, t) = 0.5$ , defined for all  $t \in [0, 3]$  and  $x$  in  $\Omega_{\text{obs}}$  of Figure 6. The penalization parameter is  $\alpha = 0.01$ . We set  $\delta_K = 1.0$  for all  $K \in \mathcal{T}_h$ . Here we have that the stabilized forms in (49) for derivatives along time for state and adjoint equations are, respectively:

$$m_s(y^{\mathcal{N}}, q^{\mathcal{N}}; \boldsymbol{\mu}) = (y^{\mathcal{N}}, q^{\mathcal{N}})_{L^2(\Omega)} + \sum_{K \in \mathcal{T}_h} \delta_K h_K (y^{\mathcal{N}}, (\cos \mu_2, \sin \mu_2) \cdot \nabla q^{\mathcal{N}})_K, \quad y^{\mathcal{N}}, q^{\mathcal{N}} \in Y^{\mathcal{N}},$$

$$m_s^*(p^{\mathcal{N}}, z^{\mathcal{N}}; \boldsymbol{\mu}) = (p^{\mathcal{N}}, z^{\mathcal{N}})_{L^2(\Omega)} - \sum_{K \in \mathcal{T}_h} \delta_K h_K (p^{\mathcal{N}}, (\cos \mu_2, \sin \mu_2) \cdot \nabla z^{\mathcal{N}})_K, \quad p^{\mathcal{N}}, z^{\mathcal{N}} \in Y^{\mathcal{N}}.$$

We consider a parameter space equal to the steady case, i.e.  $\mathcal{P} := [10^4, 10^5] \times [0, 1.57]$ . Our training set has cardinality  $N_{\text{train}} = 100$ . In Figure 10 we show a representative stabilized FEM solution for  $\boldsymbol{\mu} = (2 \cdot 10^4, 1.2)$  for some instants of time. We choose to perform a POD procedure with  $N_{\text{max}} = 30$ .

In Figure 11 one can see the relative errors of the three variables. As previously said, Only-Offline procedure has not good error behaviour. Instead, it is worth to note that in a Online-Offline



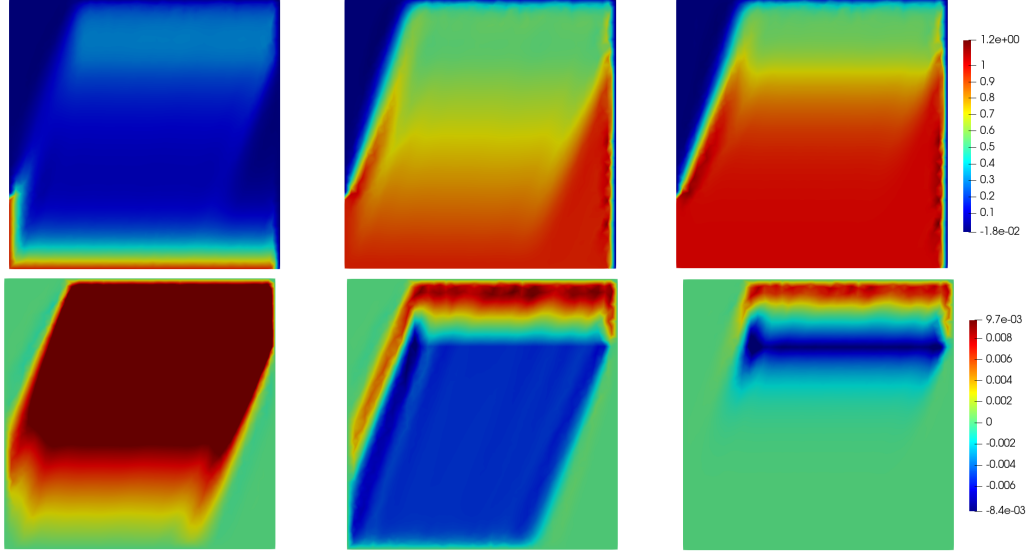


**Figure 10.** (Top) SUPG FEM state solution and (Bottom) SUPG FEM adjoint solution for  $\mu = (2 \cdot 10^4, 1.2)$  for time  $t = 0.1$  (left),  $t = 1.5$  (center),  $t = 3.0$  (right), in the Parabolic Propagating Front in a Square Problem,  $h = 0.036$ ,  $\alpha = 0.01$ ,  $\delta_K = 1.0$ .

stabilization context, errors between the FEM and the reduced solutions decrease as  $N$  grows. The fact that we deal with a two-dimensional parameter space implies to require more  $N$  basis for a good approximation of the reduced solution. We have  $e_{y,30} = 2.17 \cdot 10^{-3}$ ,  $e_{u,30} = 1.59 \cdot 10^{-3}$  and  $e_{p,30} = 5.62 \cdot 10^{-3}$ . Therefore, also for this case test we can state that the SUPG stabilization is an efficient procedure for the ROMs.

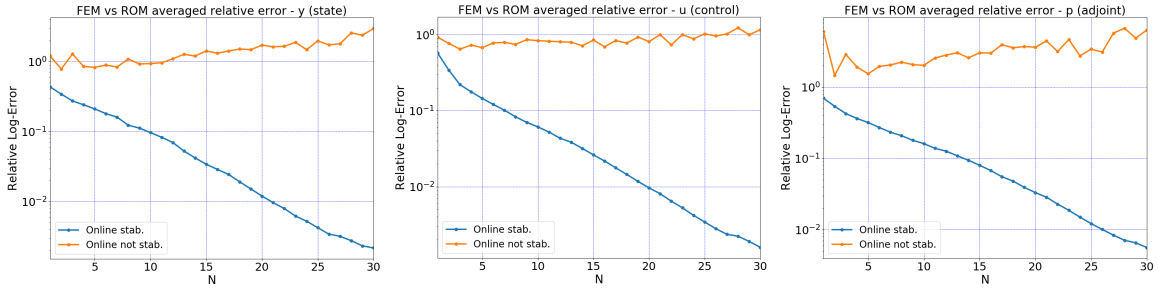


**Figure 11.** Relative errors between the FEM and the Only-Offline and Online-Offline stabilized reduced solution for the state (left), control (center) and adjoint (right) solutions, respectively with  $\mathcal{P} = [10^4, 10^5] \times [0, 1.57]$ ,  $N_t = 30$ ,  $N_{\text{test}} = 100$ ,  $\delta_K = 1.0$ ,  $h = 0.036$ .

Finally, we show the results about the speedup-index in Table 4. For  $N = 30$ , not only we have the best accuracy for the reduced problem, but we are able to computed, averagely, 3981 reduced solution in the interval of a FEM simulation. Speedup-index has an average order of magnitude of  $10^3$  overall.

## 6. CONCLUSIONS AND PERSPECTIVES

In this work, we presented the numerical experiments concerning Advection-Dominated OCPs in a ROM context with high Péclet number, both in the steady and the unsteady cases, under SUPG stabilization. Concerning ROMs, we can have two possibilities of stabilization: we can apply SUPG only to the offline phase or we can use it in both online and offline phases. We analyzed relative



$N$	Only-Offline Stabilization			Offline-Online Stabilization		
	min	average	max	min	average	max
5	6136.6	8659.4	12654.5	4588.3	6605.8	9914.7
10	6018.7	8278.8	11989.5	4282.9	6231.7	9353.3
15	5611.3	7721.4	11359.5	3725.3	5779.0	8794.3
20	4820.0	7041.2	10143.0	3567.7	5318.9	8091.1
25	3814.1	5970.5	9212.2	2751.7	4366.6	6678.3
30	3432.0	5420.1	8462.8	2424.7	3981.3	6147.9

**Table 4.** Speedup-index of the unsteady Propagating Front in a Square Problem for Online-Offline and Only-Offline stabilization with training set  $\mathcal{P} := [10^4, 10^5] \times [0, 1.57]$ ,  $h = 0.036$ ,  $\alpha = 0.01$ ,  $N_t = 30$ ,  $N_{\text{test}} = 100$ ,  $\delta_K = 1.0$ .

errors between the reduced and the high fidelity solutions and of the speedup-index concerning the Graetz-Poiseuille and Propagating Front in a Square Problems, always under a distributed control.

A  $\mathbb{P}^1$ -FEM approximation for the state, control and adjoint spaces is used in a *optimize-then-discretize* framework. Concerning parabolic problems, a space-time approach is followed and we applied in a suitable way the SUPG stabilization. For the ROM, we considered a *partitioned approach* for all three variables using the POD algorithm. In all the steady and unsteady experiments, the ROM technique performed excellently in a Online-Offline stabilization framework. Especially for parabolic problems, the speedup-index features large values thanks to the space-time formulation. Only-Offline stabilization technique performed very poorly in terms of errors, despite the little favorable speedup values. Thus, Online-Offline stabilization is preferable.

We also performed experiments inherent a geometrical parametrization and boundary control for the Graetz-Poiseuille Problem that are not shown in this work. Results were quite good for Online-Offline stabilization: we had some little oscillations regarding relative errors due to the complexity of the problem. As a perspective, it might be interesting to create a strongly-consistent stabilization technique that flattens all the fluctuation for these two configurations, since, to the best of our knowledge, this topic is still a novelty in literature.

Regarding the SUPG stabilization for parabolic OCPs in a *optimize-then-discretize* framework, it would be also worth to derive some theoretical results that gives us the accuracy of the numerical solution with respect to the time-step and the mesh-size.

In conclusion, as another goal it might be interesting to study the performance of new stabilization techniques for the online phases, such as the Online Vanishing Viscosity and the Online Rectification methods [4, 13, 33]. Moreover, the extension of this setting to the uncertainty certification context will be the topic of future research.

#### ACKNOWLEDGEMENTS

We acknowledge the support by European Union Funding for Research and Innovation – Horizon 2020 Program – in the framework of European Research Council Executive Agency: Consolidator Grant H2020 ERC CoG 2015 AROMA-CFD project 681447 “Advanced Reduced Order Methods with Applications in Computational Fluid Dynamics”. We also acknowledge the PRIN 2017 “Numerical Analysis for Full and Reduced Order Methods for the efficient and accurate solution of complex systems governed by Partial Differential Equations” (NA-FROM-PDEs) and the INDAM-GNCS project “Tecniche Numeriche Avanzate per Applicazioni Industriali”. The computations in this work have been performed with RBniCS [2] library, developed at SISSA mathLab, which is an implementation in FEniCS [32] of several reduced order modelling techniques; we acknowledge developers and contributors to both libraries.

#### REFERENCES

- [1] multiphenics - easy prototyping of multiphysics problems in FEniCS. <https://mathlab.sissa.it/multiphenics>.
- [2] RBniCS – reduced order modelling in FEniCS. <https://www.rbniicsproject.org/>.

- [3] Tuğba Akman, Bülent Karasözen, and Zahire Kanar-Seymen. Streamline Upwind/Petrov-Galerkin solution of optimal control problems governed by time-dependent diffusion-convection-reaction equations. *TWMS Journal of Applied and Engineering Mathematics*, 7(2):221–235, 2017.
- [4] Shafqat Ali. *Stabilized reduced basis methods for the approximation of parametrized viscous flows*. PhD. Thesis, SISSA, 2018.
- [5] Kendall Atkinson and Weimin Han. *Theoretical numerical analysis*, volume 39. Springer, 2005.
- [6] Francesco Ballarin, Gianluigi Rozza, and Maria Strazzullo. Chapter 9 - Space-time POD-Galerkin approach for parametric flow control. In Emmanuel Trélat and Enrique Zuazua, editors, *Numerical Control: Part A*, volume 23 of *Handbook of Numerical Analysis*, pages 307–338. Elsevier, 2022.
- [7] Roland Becker, Hartmut Kapp, and Rolf Rannacher. Adaptive finite element methods for optimal control of partial differential equations: Basic concept. *SIAM Journal on Control and Optimization*, 39(1):113–132, 2000.
- [8] Peter Benner, Mario Ohlberger, Anthony Patera, Gianluigi Rozza, and Karsten Urban. *Model reduction of parametrized systems*. Springer, 2017.
- [9] Franco Brezzi. On the existence, uniqueness and approximation of saddle-point problems arising from Lagrangian multipliers. *Publications mathématiques et informatique de Rennes*, (S4):1–26, 1974.
- [10] Franco Brezzi and Michel Fortin. *Mixed and hybrid finite element methods*, volume 15. Springer Science & Business Media, 2012.
- [11] Alexander N. Brooks and Thomas J.R. Hughes. Streamline Upwind/Petrov-Galerkin formulations for convection dominated flows with particular emphasis on the incompressible Navier-Stokes equations. *Computer methods in applied mechanics and engineering*, 32(1-3):199–259, 1982.
- [12] Giuseppe Carere. *Reduced Order Methods for Optimal Control Problems constrained by PDEs with random inputs and applications*. Master’s thesis, University of Amsterdam and SISSA, 2019.
- [13] Rachida Chakir, Yvon Maday, and Philippe Parnaudeau. A non-intrusive reduced basis approach for parametrized heat transfer problems. *Journal of Computational Physics*, 376:617–633, 2019.
- [14] S. Scott Collis and Matthias Heinkenschloss. Analysis of the Streamline Upwind/Petrov Galerkin method applied to the solution of optimal control problems. *CAAM TR02-01*, 108, 2002.
- [15] Luca Dedè. Reduced Basis Method and A Posteriori Error Estimation for Parametrized Linear-Quadratic Optimal Control Problems. *SIAM Journal on Scientific Computing*, 32(2):997–1019, 2010.
- [16] Kenneth Eriksson and Claes Johnson. Error estimates and automatic time step control for nonlinear parabolic problems, I. *SIAM journal on numerical analysis*, 24(1):12–23, 1987.
- [17] Sashikumaar Ganesan. An operator-splitting Galerkin/SUPG finite element method for population balance equations: stability and convergence. *ESAIM: Mathematical Modelling and Numerical Analysis*, 46(6):1447–1465, 2012.
- [18] Fabrizio Gelsomino and Gianluigi Rozza. Comparison and combination of reduced-order modelling techniques in 3D parametrized heat transfer problems. *Mathematical and Computer Modelling of Dynamical Systems*, 17(4):371–394, 2011.
- [19] Anna-Lena Gerner and Karen Veroy. Certified Reduced Basis Methods for Parametrized Saddle Point Problems. *SIAM Journal on Scientific Computing*, 34(5):A2812–A2836, 2012.
- [20] Svetlana Giere, Traian Iliescu, Volker John, and David Wells. SUPG reduced order models for convection-dominated convection–diffusion–reaction equations. *Computer Methods in Applied Mechanics and Engineering*, 289:454–474, 2015.
- [21] Rafaela Guberovic, Christoph Schwab, and Rob Stevenson. Space-time variational saddle point formulations of Stokes and Navier–Stokes equations. *ESAIM: Mathematical Modelling and Numerical Analysis*, 48(3):875–894, 2014.
- [22] Jan S. Hesthaven, Gianluigi Rozza, and Benjamin Stamm. *Certified reduced basis methods for parametrized partial differential equations*, volume 590. Springer, 2016.
- [23] Michael Hinze, Michael Köster, and Stefan Turek. A hierarchical space-time solver for distributed control of the Stokes equation. *Technical Report, SPP1253-16-01*, 2008.
- [24] Michael Hinze, René Pinnau, Michael Ulbrich, and Stefan Ulbrich. *Optimization with PDE constraints*, volume 23. Springer Science & Business Media, 2008.
- [25] Thomas J.R. Hughes. A multidimensional upwind scheme with no crosswind diffusion. *Finite Element Methods for Convection Dominated Flows, AMD 34*, 1979.
- [26] Thomas J.R. Hughes. Recent progress in the development and understanding of SUPG methods with special reference to the compressible Euler and Navier-Stokes equations. *International journal for numerical methods in fluids*, 7(11):1261–1275, 1987.
- [27] Volker John and Julia Novo. Error analysis of the SUPG finite element discretization of evolutionary convection-diffusion-reaction equations. *SIAM journal on numerical analysis*, 49(3):1149–1176, 2011.
- [28] Mark Kärcher, Zoi Tokoutsis, Martin A. Grepl, and Karen Veroy. Certified reduced basis methods for parametrized elliptic optimal control problems with distributed controls. *Journal of Scientific Computing*, 75(1):276–307, 2018.
- [29] Karl Kunisch and Stefan Volkwein. Proper orthogonal decomposition for optimality systems. *ESAIM: Mathematical Modelling and Numerical Analysis*, 42(1):1–23, 2008.
- [30] Jacques-Louis Lions. *Optimal control of systems governed by partial differential equations*, volume 170. Springer Verlag, 1971.

- [31] Jacques-Louis Lions. *Some aspects of the optimal control of distributed parameter systems*. SIAM, 1972.
- [32] Anders Logg, Kent-Andre Mardal, and Garth Wells. *Automated solution of differential equations by the finite element method: The FEniCS book*, volume 84. Springer Science & Business Media, 2012.
- [33] Yvon Maday and Eitan Tadmor. Analysis of the spectral vanishing viscosity method for periodic conservation laws. *SIAM Journal on Numerical Analysis*, 26(4):854–870, 1989.
- [34] Federico Negri. *Reduced basis method for parametrized optimal control problems governed by PDEs*. Master’s thesis, Politecnico di Milano and EPFL, 2011.
- [35] Federico Negri, Andrea Manzoni, and Gianluigi Rozza. Reduced basis approximation of parametrized optimal flow control problems for the Stokes equations. *Computers & Mathematics with Applications*, 69(4):319–336, 2015.
- [36] Federico Negri, Gianluigi Rozza, Andrea Manzoni, and Alfio Quarteroni. Reduced basis method for parametrized elliptic optimal control problems. *SIAM Journal on Scientific Computing*, 35(5):A2316–A2340, 2013.
- [37] Paolo Pacciarini and Gianluigi Rozza. Stabilized reduced basis method for parametrized advection–diffusion PDEs. *Computer Methods in Applied Mechanics and Engineering*, 274:1–18, 2014.
- [38] Alfio Quarteroni. *Numerical models for differential problems*, volume 2. Springer, 2009.
- [39] Alfio Quarteroni, Andrea Manzoni, and Federico Negri. *Reduced basis methods for partial differential equations: an introduction*, volume 92. Springer, 2015.
- [40] Alfio Quarteroni, Gianluigi Rozza, et al. *Reduced order methods for modeling and computational reduction*, volume 9. Springer, 2014.
- [41] Alfio Quarteroni, Gianluigi Rozza, and Andrea Manzoni. Certified reduced basis approximation for parametrized partial differential equations and applications. *Journal of Mathematics in Industry*, 1(1):1–49, 2011.
- [42] Alfio Quarteroni and Alberto Valli. *Numerical approximation of partial differential equations*, volume 23. Springer Science & Business Media, 2008.
- [43] Gianluigi Rozza, Dinh Bao Phuong Huynh, and Anthony T. Patera. Reduced basis approximation and a posteriori error estimation for affinely parametrized elliptic coercive partial differential equations. *Archives of Computational Methods in Engineering*, 15(3):229–275, 2008.
- [44] Gianluigi Rozza, Ngoc-Cuong Nguyen, Anthony T. Patera, and Simone Deparis. Reduced basis methods and a posteriori error estimators for heat transfer problems. In *Heat Transfer Summer Conference*, volume 43574, pages 753–762, 2009.
- [45] Z. Kanar Seymen, Hamdullah Yücel, and Bülent Karasözen. Distributed optimal control of time-dependent diffusion–convection–reaction equations using space–time discretization. *Journal of Computational and Applied Mathematics*, 261:146–157, 2014.
- [46] Martin Stoll and Andrew J. Wathen. All-at-once solution of time-dependent PDE-constrained optimization problems. *Unspecified, Tech. Rep*, 2010.
- [47] Martin Stoll and Andy Wathen. All-at-once solution of time-dependent Stokes control. *Journal of Computational Physics*, 232(1):498–515, 2013.
- [48] Maria Strazzullo. *Model Order Reduction for Nonlinear and Time-Dependent Parametric Optimal Flow Control Problems*. PhD. Thesis, SISSA, 2021.
- [49] Maria Strazzullo, Francesco Ballarin, Renzo Mosetti, and Gianluigi Rozza. Model reduction for parametrized optimal control problems in environmental marine sciences and engineering. *SIAM Journal on Scientific Computing*, 40(4):B1055–B1079, 2018.
- [50] Maria Strazzullo, Francesco Ballarin, and Gianluigi Rozza. POD-Galerkin model order reduction for parametrized time dependent linear quadratic optimal control problems in saddle point formulation. *Journal of Scientific Computing*, 83:1–35, 2020.
- [51] Maria Strazzullo, Francesco Ballarin, and Gianluigi Rozza. A certified reduced basis method for linear parametrized parabolic optimal control problems in space-time formulation. *arXiv preprint arXiv:2103.00460*, 2021.
- [52] Maria Strazzullo, Francesco Ballarin, and Gianluigi Rozza. Pod-Galerkin model order reduction for parametrized nonlinear time-dependent optimal flow control: an application to shallow water equations. *Journal of Numerical Mathematics*, 30(1):63–84, 2022.
- [53] Timothy John Sullivan. *Introduction to Uncertainty Quantification*, volume 63. Springer, 2015.
- [54] Davide Torlo. *Stabilized reduced basis method for transport PDEs with random inputs*. Master’s thesis, University of Trieste and SISSA, 2016.
- [55] Davide Torlo, Francesco Ballarin, and Gianluigi Rozza. Stabilized weighted reduced basis methods for parametrized advection dominated problems with random inputs. *SIAM/ASA Journal on Uncertainty Quantification*, 6(4):1475–1502, 2018.
- [56] Fredi Tröltzsch. *Optimal control of partial differential equations: theory, methods, and applications*, volume 112. American Mathematical Soc., 2010.
- [57] Karsten Urban and Anthony T. Patera. A new error bound for reduced basis approximation of parabolic partial differential equations. *Comptes Rendus Mathématique*, 350(3-4):203–207, 2012.
- [58] Luca Venturi. *Weighted Reduced Order Methods for parametrized PDEs in uncertainty quantification problems*. Master’s thesis, University of Trieste and SISSA, 2016.